

To appear in The Astronomical Journal

Evidence for a New Elliptical-Galaxy Paradigm: Sérsic and Core Galaxies

I. Trujillo

Max-Planck-Institut für Astronomie, Königstuhl 17, D-69117 Heidelberg, Germany

`trujillo@mpia-hd.mpg.de`

and

Peter Erwin, A. Asensio Ramos

Instituto de Astrofísica de Canarias, Calle Vía Láctea s/n, E-38200 La Laguna, Tenerife, Spain

`erwin@ll.iac.es, aasensio@ll.iac.es`

and

Alister W. Graham

Department of Astronomy, P.O. Box 112055, University of Florida, Gainesville, FL 32611

`graham@astro.ufl.edu`

ABSTRACT

We fit the surface-brightness profiles of 21 elliptical galaxies using both the Sérsic function and a new empirical model which combines an inner power law with an outer Sérsic function. The profiles are combinations of deconvolved *HST* profiles from the literature and ellipse fits to the full WFPC2 mosaic images, and thus span a radial range from $\sim 0''.02$ to \sim twice the half-light radius. We are able to accurately fit the entire profiles using either the Sérsic function or our new model. In doing so, we demonstrate that most, if not all, so-called “power-law” galaxies are better described as “Sérsic galaxies” — they are well modeled by the three-parameter Sérsic profile into the limits of *HST* resolution — and that “core” galaxies are best understood as consisting of an outer Sérsic profile with an inner power-law cusp, which is a downward deviation from the inward extrapolation of the Sérsic profile. This definition of cores resolves ambiguities that result when the popular “Nuker law” is fitted to the profiles of ellipticals and bulges, particularly at lower luminosities. We also find that using the Nuker law to model core-galaxy nuclear profiles systematically overestimates the core radii by factors of 1.5–4.5 and underestimates the inner power-law slope by ~ 20 –40% or more.

Subject headings: galaxies: elliptical and lenticular, cD — galaxies: fundamental parameters — galaxies: nuclei — galaxies: photometry — galaxies: structure

1. Introduction

The availability of high-resolution imaging with the *Hubble Space Telescope* (*HST*) has revolutionized the study of galaxy centers. Following up on early work by Crane et al. (1993), Kormendy et al. (1994), Grillmair et al. (1994), Jaffe et al. (1994), and Ferrarese et al. (1994), a series of papers by the “Nuker team” (Lauer et al. 1995; Byun et al. 1996; Gebhardt et al. 1996; Faber et al. 1997) presented a detailed study of the central regions of early-type galaxies (specifically, ellipticals and the bulges of spiral galaxies). They introduced a model for fitting the radial surface-brightness profiles: a double power-law with an adjustable transition region, dubbed the “Nuker law”:

$$I(r) = I_b 2^{(\beta-\gamma)/\alpha} \left(\frac{r}{r_b} \right)^{-\gamma} \left[1 + \left(\frac{r}{r_b} \right)^\alpha \right]^{(\gamma-\beta)/\alpha}. \quad (1)$$

The inner and outer power law exponents are γ and β , respectively; I_b is the surface brightness at the core or “break” radius r_b , and α controls the sharpness of the transition between the two power laws (larger α = sharper transition). They identified two distinct classes of galaxy centers: “power-law” galaxies, where the central surface brightness increases into the limit of resolution with something like a steep power-law profile; and “core” galaxies, where the luminosity profile turns over at a fairly sharp “break radius” into a shallower power-law. Ferrarese et al. and Faber et al. found evidence that global parameters of early-type galaxies correlated with their nuclear profiles: core galaxies tend to have high luminosities, boxy isophotes, and pressure-supported kinematics, while power-law galaxies are typically lower-luminosity and often have disk isophotes and rotationally supported kinematics.

The Nuker-law parameterization of galaxy centers has subsequently enjoyed a great deal of popularity, including extensive studies using WFPC2 and NICMOS (e.g., Rest et al. 2001; Quillen, Bowen, & Stritzinger 2000; Ravindranath et al. 2001; Laine et al. 2003), and extensions to early- and late-type spirals (e.g., Carollo & Stiavelli 1998; Seigar et al. 2002). These more recent studies have, however, suggested that the clear core/power-law dichotomy found by the Nuker team may not be so clear after all. In addition, almost all the studies using *HST* data and Nuker-law fits have left unanswered a key question: how does the nuclear part of a bulge or elliptical, seemingly well fit by a double power-law, connect to the outer profiles of such systems, which are generally well fit by the Sérsic (1968) $r^{1/n}$ function? In our first paper (Graham et al. 2003a, hereafter Paper I), we discussed some of the systematic problems and ambiguities which can arise when using a double power-law model to fit galaxy light profiles, and suggested a new hypothesis and a new model which might resolve some of these problems. The hypothesis has two parts: first, that the nuclear (*HST*-resolved) profiles of most lower-luminosity hot systems, including the power-law galaxies, are simply inward extensions of each galaxy’s outer profile, best modeled with a Sérsic function;

second, that core galaxies are best modeled with our new function, an outer Sérsic function with a break to an inner power-law. In this paper, we make an empirical test of this proposed solution, by modeling the *entire* light profiles of a sample of elliptical galaxies.

In what follows, we first review some of the problems stemming from the use of the Nuker law, including the problem of how best to identify genuine cores in galaxies (Section 2); readers familiar with these issues can probably skip this section. We then discuss our sample selection, data reduction and analysis, and the source of the profiles used (Section 3). In Section 4, we discuss the Sérsic model and our new model for core-galaxy profiles. Section 5 presents criteria for identifying core galaxies, and for discriminating between core and Sérsic profiles. We also present the results of our fits to the galaxy profiles and compare their fidelity to the profiles with that of the Nuker-law fits. Some of the implications are discussed in Section 6, and we conclude with a brief summary in Section 7. Finally, several useful mathematical expressions related to our new model are presented in the Appendix.

2. Some Outstanding Issues

2.1. Relating Nuclear Surface Brightness Profiles to Outer Profiles

The progress engendered by the use of *HST* data and the Nuker law has tended to encourage a disconnect between the inner and outer regions of galaxies, which are studied separately and parameterized in different fashions. This is in part due to the fact that early *HST* studies using the first-generation Planetary Camera generally provided useful data only for $r \lesssim 10''$ (e.g. Lauer et al. 1995), so that only the nuclear region could be studied. But it is also due to the fact that the Nuker law does *not* describe the light profiles outside this region well, even for “single-component” galaxies like ellipticals (e.g., Byun et al. 1996).

Meanwhile, there has been significant progress in understanding the luminosity structure *outside* the nuclear regions. These “global” surface brightness profiles are usually well described with Sérsic’s (1968) $r^{1/n}$ law, a generalization of de Vaucouleurs’ (1959) $r^{1/4}$ law. This has been shown to be true for both luminous ellipticals (e.g., Capaccioli 1987; Caon, Capaccioli, & D’Onofrio 1993; Graham et al. 1996) and dwarf ellipticals (e.g., Davies et al. 1988; Cellone, Forte, & Geisler 1994; Young & Currie 1994; Durrell 1997; Binggeli & Jerjen 1998; Graham & Guzmán 2003) and for the bulges of disk galaxies (Andredakis, Peletier, & Balcells 1995; Seigar & James 1998; Khosroshahi, Wadadekar, & Kembhavi 2000; Graham 2001; Balcells et al. 2003; MacArthur, Courteau, & Holtzman 2003). There is now good evidence that the *shape* of the overall surface-brightness profile, as parameterized by the Sérsic index n , correlates with numerous (model-independent) elliptical and bulge properties: the total luminosity, the central surface brightness, the effective radius, and the central velocity dispersion (Graham, Trujillo, & Caon 2001a; Möllenhoff & Heidt 2001; Graham 2002). It also correlates extremely well with the mass of central supermassive black holes (Graham et al. 2001b; Erwin, Caon, & Graham 2003). This clearly points to connections between the global

distribution of stars in ellipticals and bulges and the properties of their nuclear regions, and makes it more important than ever to understand how the nuclear regions connect to the outer parts of galaxies.

2.2. The Ambiguity of Current Core and Power-law Definitions

A second problem is the ambiguity of “core” versus “power-law” definitions, and the apparent unraveling of the clear distinction between (high-luminosity) core and (lower-luminosity) power-law galaxies reported by Faber et al. (1997). Rest et al. (2001) and Ravindranath et al. (2001) have found several examples of “intermediate” galaxies ($0.3 < \gamma < 0.5$; see, e.g., Fig. 3 of Ravindranath et al.); it is not clear where these galaxies fit into the core/power-law scheme. Taking a slightly different tack, Carollo et al. (1997) argued for a general trend of γ versus absolute magnitude for ellipticals, with more luminous galaxies having shallower slopes: this roughly matches the trend found by Faber et al. 1997, but without splitting the galaxies into core and power-law categories. However, subsequent investigation of lower-luminosity systems, particularly bulges in late-type galaxies and dwarf ellipticals, has shown a *reversal* of this trend: for low-luminosity systems, luminosity and inner power-law slope are *anti*-correlated (Stiavelli et al. 2001, especially their Fig. 4). This has also been portrayed as a dichotomy between more luminous “ $R^{1/4}$ ” bulges, with high γ , and less luminous “exponential” bulges, which tend to have $\gamma < 0.3$ (Seigar et al. 2002).

To dramatize this problem, we plot γ versus M_B in Figure 1 for ellipticals spanning a wide range of absolute magnitudes, from the brightest core galaxies of Faber et al. (1997) down to the faint dwarf ellipticals of Stiavelli et al. (2001); a similar figure can be found in Graham & Guzmán (2003). We indicate the boundaries for core and power-law galaxies, according to Faber et al. (1997); all galaxies plotted have well-resolved “cores” ($r_b \geq 0''.16$). Two things stand out: first, there are numerous “intermediate” objects, so that the rather clear distinction reported by Faber et al. — that systems with small γ are high luminosity, while systems with large γ are lower luminosity — has become murky. Second, if we apply the standard definition of a core, then fully 21 of the 25 dwarf ellipticals of Stiavelli et al. (2001) have cores! Similarly, 12 of 38 spiral bulges (not plotted) studied in the optical by Carollo & Stiavelli (1998) and 10 of 45 bulges studied in the near-IR by Seigar et al. (2002) meet the standard criteria for having cores.¹ Either both low- and high-luminosity galaxies — but *not* intermediate-luminosity systems — have cores, or we need a less problematic way of identifying cores.

As we showed in Paper I, this kind of ambiguity arises automatically if the surface-brightness profile is exponential or nearly so (i.e., a Sérsic function with $n \lesssim 2$): when plotted in log-log space — and when fit with a double power-law such as the Nuker law — such profiles will seem to have

¹Note that these authors do not classify centers into core/power-law categories, and so do not actually label these “core” galaxies.

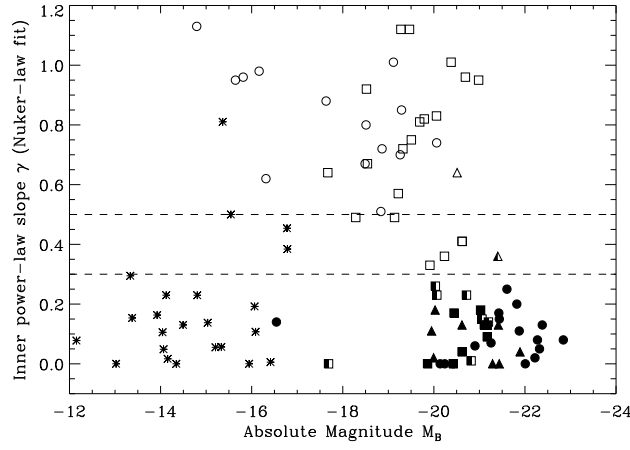


Fig. 1.— The problem of how to identify “cores”: inner logarithmic slope γ , from Nuker-law fits to *HST* profiles, versus absolute magnitude M_B for dwarf ellipticals from Stiavelli et al. (2001, asterisks) and regular ellipticals from Faber et al. (1997, circles), Rest et al. (2001, boxes), and Ravindranath et al. (2001, triangles). Filled symbols are core galaxies and half-filled symbols are “intermediate” galaxies, according to the authors of each study; Stiavelli et al. do not make core/non-core classifications. Total B magnitudes are from LEDA, distances are from Tonry et al. (2001) or LEDA (corrected for Virgo infall and assuming $H_0 = 75 \text{ km s}^{-1} \text{ kpc}^{-1}$); for Virgo cluster galaxies without measured distances, we assume $D = 15.3 \text{ Mpc}$ (Freedman et al. 2001). Only galaxies with Nuker-fit break radii $r_b \geq 0''.16$ are plotted, so all galaxies with $\gamma < 0.3$ (lower dashed line) are “core” galaxies according to the standard definition (Lauer et al. 1995; Faber et al. 1997); galaxies with $\gamma > 0.5$ (upper dashed line) are “power-law” galaxies in the same scheme.

cores. Since dwarf ellipticals and the bulges of many galaxies have profiles which are well fit by Sérsic functions with small n (see references above), this is clearly a concern. The argument that Sérsic profiles only apply to the *outer* parts of profiles (that is, outside the region typically imaged by *HST*) is not tenable. Geha, Guhathakurta, & van der Marel (2002) and Graham & Guzmán (2003) were able to fit the *HST* profiles of dwarf ellipticals using Sérsic profiles (plus optional nuclear components). In addition, Jerjen et al. (2000) found that the fully resolved surface-brightness profiles of Local Group dwarf spheroidals — which they show to be primarily the low-luminosity extension of the dwarf ellipticals — are quite well fit by Sérsic profiles (see also Caldwell 1999).

Since the Sérsic shape parameter n is correlated with luminosity (e.g., Caon, Capaccioli, & D’Onofrio 1993; Jerjen et al. 2000; Graham & Guzmán 2003) and with central velocity dispersion (Graham, Trujillo, & Caon 2001a; Graham 2002), we have a natural explanation for the correlation between γ and luminosity: Sérsic profiles observed from the ground continue inward into the regions resolved by *HST*, so that galaxies with larger n (higher luminosities) will have larger² γ . Figure 2 shows that this is supported by the Sérsic fits and γ measurements of Stiavelli et al. (2001): dwarf ellipticals with larger values of n have larger values of γ , in line with what we expect from Sérsic profiles observed at small radii. In Section 5 we show that the inner regions of higher-luminosity, power-law ellipticals (high γ) are well fit by Sérsic functions with large n which simultaneously fit the outer profiles.

But where does that leave core galaxies? The results of Gebhardt et al. (1996) and Faber et al. (1997) strongly suggest that the low- γ cores identified in these galaxies are genuine, physically distinct structures; indeed, some of these cores were well-known from high-resolution, ground-based imaging (e.g., Kormendy 1985; Lauer 1985; see the discussion in Lauer et al. 1995). The outer profiles of *high*-luminosity ellipticals, those most likely to have such cores, have large values of n , so the inner slope γ should be large, the opposite of what is observed. This means that cores in bright ellipticals are clear deviations from the outer (Sérsic) profiles, and suggests a more natural way of identifying cores: a downward *deviation*, with shallow logarithmic slope, from a galaxy’s outer Sérsic profile. This would resolve the ambiguity we noted above: illusory “cores” in low-luminosity systems (produced by fitting a double-power law to low- n Sérsic profiles) cannot be confused with *true* cores in high-luminosity systems. In Section 5, we show that this is indeed a viable approach: the complete profiles of high-luminosity *core* galaxies are *not* well fit by a single Sérsic profile, but *are* well fit by our new model, which joins a single, inner power-law profile to an outer Sérsic profile.

²Eq. A15 shows the relation between γ and n for a Sérsic profile.

3. Sample Selection, Data Reduction, and Generation of Profiles

3.1. Sample Selection

For this study, we needed a set of galaxies with *HST* observations of their central regions, as well as observations of the outer parts of the galaxies. Ideally, we want to compare our results with those of previous studies which used Nuker-law fits to analyze and classify the galaxies. This drove us to concentrate on the two largest *HST* studies of early-type galaxies: the WF/PC1 study of the Nuker team (Lauer et al. 1995; Byun et al. 1996), and Rest et al. (2001), which used WFPC2. In both cases, the authors presented deconvolved profiles derived from ellipse fits to the Planetary Camera chips; Rest et al. (2001) also present values at very small radii derived directly from individual pixel values. Since these are the data which the Nuker team and Rest et al. use for their Nuker-law fits and classifications, it made sense for us to use them as well.

The problem then became finding suitable profiles for the galaxies outside the region imaged by the PC chips ($r \gtrsim 20''$). To minimize problems which might arise from combining profiles from different filters, we needed *V*-band images to go with the F555W profiles from Lauer et al. (1995) and *R*-band images to go with the F702W profiles from Rest et al. (2001). We also wanted images with fairly high resolution, to avoid any possible changes in curvature induced by trying to match ground-based profiles with poor seeing to the high-resolution *HST* images. The simplest solution to both of these requirements was to use *HST* images — in particular, WFPC2 images obtained using the same filters. Although the WFPC2 array is missing almost a quarter of its field, the overall field of view is $\approx 2.6'$, which is sufficient to cover smaller galaxies; for larger galaxies, we can still sample most of the profile with the ellipse fits. In addition, the very low background in *HST* images means that we are less vulnerable to sky subtraction errors, which can affect the outer profiles. In practice, we found the following restrictions worked best: major axis $< 4'$ and minor axis $< 3'$, using the $\mu_B = 25$ dimensions from de Vaucouleurs et al. (1991, hereafter RC3).

The decision to use *HST* images makes the match with the inner profiles of Rest et al. (2001) particularly good: it means that we are using the exact same F702W images they used. For the F555W profiles of the Nuker team, we searched the *HST* archive for WFPC2 images in the same filter (the F555W filters of the two cameras are not precisely identical, but the differences are too small to matter). There were somewhat fewer of these, so most of the galaxies we analyze are from the Rest et al. sample.

Finally, we decided to examine only elliptical galaxies. Although the bulges of disk galaxies are known to be well fit by the Sérsic model, extracting the actual bulge profile means making bulge-disk decompositions. While not a significant problem for some galaxies, it does add some uncertainty, since we could end up fitting a one-dimensional profile with as many as *eight* free parameters (disk scale length and central surface brightness + five or six parameters for our new model). In the future, we do plan to analyze the bulges of disk galaxies using our new model, but for the purposes of this study we wanted to simplify matters and eliminate as much ambiguity as

possible.

Thus, we selected only elliptical galaxies from the samples of the Nuker team and Rest et al. (2001). This meant not just selecting those galaxies classified as elliptical, but also ensuring that they were, in fact, true ellipticals with no significant disk component. A number of nominal E galaxies showed signs of having significant outer disks, suggesting that they may well be misclassified E/S0 or S0 galaxies. Our criteria included kinematic evidence from the literature, ellipse fits to the WFPC2 mosaic images, bulge+disk decompositions using the extra-nuclear ($r > 1''$) part of the profiles, and the presence of substructures such as rings and bars, which are evidence for disks massive enough to be self-gravitating. Appendix C discusses rejected galaxies on a case-by-case basis. The remaining 21 galaxies, which we judged to be bona-fide ellipticals, are listed in Table 1.

The angular size limits and the nature of the previous samples we draw on mean that the galaxies in Table 1 span a limited range in absolute magnitude. Happily, this narrow magnitude range ends up bracketing the overlap between core and power-law galaxies, and we have roughly equal numbers of each.

3.2. Data Reduction and Profile Matching

The WFPC2 images were retrieved from the *HST* archive with standard on-the-fly calibration. Multiple exposures were combined using the `crrej` task within IRAF. Alignment of different exposures was checked using coordinates of bright stars and galaxy nuclei; if the offset was $\lesssim 0.2$ pixels in the PC chip, then the images were combined without shifting. (Since we use the published profiles of Lauer et al. 1995 and Rest et al. 2001 for $r \lesssim 10''$, we do not need highly accurate alignment.) We then made mosaic images from the combined exposures using the `wmosaic` task. Sky subtraction was based on the average of median values from several 10×10 pixel boxes, located well away from the galaxy. In some cases, there was evidence that galaxy light was present even at the edges of the WF chips, so the outermost one or two points in the profiles may not be very reliable (the effect appears to be significant only for NGC 2986).

We derived surface-brightness profiles from the sky-subtracted mosaic images by fitting ellipses to the isophotes with the IRAF task `ellipse`, using logarithmic spacing and median filtering. The mosaic images were first masked to exclude the missing quadrant and the gaps between the individual chips, as well any bright foreground stars or other galaxies. Results of ellipse fits are shown in Appendix B.

The resulting major-axis profiles were then combined with the published, deconvolved major-axis profiles for the inner regions, from Lauer et al. (1995) and Rest et al. (2001); these inner profiles typically extend to semi-major axis $a \approx 10\text{--}20''$. We matched our outer, mosaic-based profiles to these inner profiles using the overlap at $2'' \leq a \leq 10''$. This is sufficiently outside the center that differences due to resolution effects are minimized. The profile from the mosaic was only used for radii outside the literature profiles, except for some of the profiles from Rest et al.,

Table 1. The galaxy sample and global parameters

Galaxy (1)	Type (2)	B_T (3)	M_B (4)	Distance (5)	source (6)	V_{vir} (7)	Innermost Data (8)	σ (9)	Profile Type (10)
NGC 1426	E4	12.62	-19.29	24.1	3	1232	0''25 / 29.2 pc	155	\
NGC 1700	E4	11.87	-21.36	44.3	3	3800	0.09 / 19.3	243	\
NGC 4458	E0-1	12.86	-18.32	17.2	3	768	0.13 / 10.8	106	\
NGC 5845	E:	13.24	-18.83	25.9	3	1634	0.02 / 2.8	244	\
From Rest et al. (2001)									
NGC 2634	E1:	12.93	-19.69	33.4	3	2539	0.10 / 16.2	172	\
NGC 2872	E2	12.67	-20.44	41.9	4	3143	0.49 / 99.5	284	\
NGC 2986	E2	11.41	-20.89	28.9	4	2170	0.02 / 2.8	260	\cap
NGC 3078	E2-3	11.75	-20.98	35.2	3	2339	0.63 / 108	237	\
NGC 3348	E0	11.71	-21.36	41.2	4	3092	0.02 / 4.0	239	\cap
NGC 3613	E6	11.70	-20.62	29.1	3	2246	0.05 / 7.1	205	\cap
NGC 4168	E2	12.00	-20.45	30.9	3	2396	0.12 / 18.0	186	\cap
NGC 4291	E3	12.23	-19.40	26.2	3	2047	0.04 / 5.1	278	\cap
NGC 4478	E2	12.07	-19.22	18.1	3	1485	0.02 / 1.8	143	\
NGC 5017	E+?	13.18	-19.43	33.3	4	2495	0.33 / 53.3	174	\
NGC 5077	E3-4	12.12	-20.70	36.7	4	2752	0.14 / 24.9	273)
NGC 5557	E1	11.96	-21.34	45.7	4	3427	0.02 / 4.4	259)
NGC 5576	E3	11.80	-20.23	25.5	3	1565	0.02 / 2.5	190	\
NGC 5796	E0-1	12.36	-20.61	39.3	4	2950	0.02 / 3.8	290	\
NGC 5831	E3	12.62	-19.55	27.2	3	1740	0.02 / 2.6	168	\
NGC 5903	E2	11.48	-21.17	33.9	3	2466	0.02 / 3.3	217	\cap
NGC 5982	E3	11.88	-21.25	42.2	4	3168	0.02 / 4.1	256	\cap

Note. — Global parameters for the galaxies in our sample: Col. (1): Galaxy name. Col. (2): Morphological type from RC3. Col. (3): Total apparent B -band magnitude, corrected for Galactic extinction and redshift, from LEDA (see Paturel et al. 1997). Col. (4): Absolute B -band magnitude, using distance from column 5. Col. (5): Distance in Mpc. Col. (6): Sources for the distances: 3 = SBF distance from Tonry et al. (2001), 4 = corrected radial velocity (col. [7]) and $H_0 = 75 \text{ km s}^{-1} \text{ kpc}^{-1}$. Col. (7): Radial velocity (in km s^{-1}), corrected for Virgocentric infall, from LEDA (infall model in Paturel et al. 1997). Col. (8): Radius of innermost data point used in fits, in arc seconds and in parsecs. Col. (9): Central velocity dispersion in km s^{-1} , from McElroy (1995). Col. (10): Original *HST* inner profile classification from Nuker-law fits, from either Lauer et al. (1995) or Rest et al. (2001); \,), and \cap indicate power-law, intermediate, and core galaxies, respectively.

where we added points from the mosaic profile to fill in gaps in their profiles at $r > 2''$, to create composite profiles that were more evenly spaced in logarithmic radius. For the Rest et al. profiles, we attempted to sample the inner part of their profiles with approximately the same spacing as our mosaic profiles, again with the aim of producing composite profiles that are more-or-less evenly spaced in logarithmic radius. If the original studies excluded values at small radii from the fits (as indicated by Figure 3 of Byun et al. 1996 and Figure 8 of Rest et al.) — due to the presence of distinct nuclei or strong dust absorption — then we also excluded those points.³ The combined profiles can be seen in Section 5.

4. Models for Galaxy Light Profiles

The Sérsic (1968) model can be defined as:

$$I(r) = I(0) \exp[-b_n(r/r_e)^{1/n}], \quad (2)$$

with $I(0)$ being the central intensity, r_e the scale radius (= half-light radius), and n the shape parameter controlling the overall curvature; when $n = 1$, this reduces to an exponential, while $n = 4$ gives the traditional de Vaucouleurs (1959) $r^{1/4}$ profile. The quantity b_n is a function of the shape parameter n , chosen to ensure that the scale radius encloses half of the total luminosity. The evaluation of b_n can be found in Eqn. A7.

Our new model, introduced in Paper I and Graham et al. (2003c), is analogous to the Nuker law, but uses the Sérsic model for the outer part of the profile (see Paper I for some representative plots). This model, which we will refer to as “core-Sérsic,” is

$$I(r) = I' \left[1 + \left(\frac{r_b}{r} \right)^\alpha \right]^{\gamma/\alpha} \exp \left[-b \left(\frac{r^\alpha + r_b^\alpha}{r_e^\alpha} \right)^{1/(n\alpha)} \right], \quad (3)$$

with

$$I' = I_b 2^{-\gamma/\alpha} \exp[b 2^{1/\alpha n} (r_b/r_e)^{1/n}]. \quad (4)$$

The parameters have the same general meaning as in the Sérsic or Nuker laws: the break radius r_b is the point at which the profile changes from one regime to another, γ is the slope of the inner power law region, I_b is the intensity at the break radius, α controls the sharpness of the transition between the cusp and the outer Sérsic profile, r_e is the effective radius of the profile, and n is the shape parameter of the outer Sérsic part. The quantity b is a function of the parameters α , r_b/r_e , γ , and n , and is defined in such a way that r_e becomes the radius enclosing half the light of the galaxy model (see Appendix A). If $\alpha \rightarrow \infty$, then the transition from Sérsic profile to power law at

³The exception is NGC 5845, where we were only able to reproduce the original Nuker-law fit (and rms residuals) of Byun et al. by including *all* of the inner points.

r_b is infinitely sharp, with no transition region. In this limiting case, the model can be written as:

$$I(r) = I_b \left[\left(\frac{r_b}{r} \right)^\gamma u(r_b - r) + e^{b(r_b/r_e)^{1/n}} e^{-b(r/r_e)^{1/n}} u(r - r_b) \right], \quad (5)$$

with $u(x - a)$ being the Heaviside step function. Eq. 5 can also be approximated using Eq. 3 with $\alpha \gtrsim 100$. Carollo & Stiavelli (1998) introduced a more limited version of Eqn. 3, with a non-adjustable transition region and an exponential instead of the Sérsic outer region. (They used it to model — generally without success — the profiles of low-luminosity, “exponential” bulges with nuclear excesses, rather than those of the higher-luminosity ellipticals which typically have cores.)

For the $\alpha \rightarrow \infty$ case, the relation between the intensity at the effective radius r_e and the intensity at the break radius r_b , assuming that $r_e > r_b$, is given by:

$$I(r_e) = I_b \exp[b((r_b/r_e)^{1/n} - 1)] \quad (6)$$

or, equivalently,

$$\mu_e = \mu_b - 2.5b((r_b/r_e)^{1/n} - 1) \log e. \quad (7)$$

The definition for b in the general case (α = free) is somewhat complex, though the necessary integrations can be done numerically beforehand and interpolated for actual fitting.⁴ A simpler, mathematically equivalent version can be had if we replace b by b_n from the Sérsic model, in which case $r_e \rightarrow r_{es}$, the half-light radius of the outer Sérsic profile (i.e., considered as a complete Sérsic profile extending in to $r = 0$).⁵ For unrealistically large cores (inner power-law regions), this r_{es} (and its corresponding μ_{es}) will not be a good approximation to the true r_e and μ_e of the profile. In practice, as long as $r_b \ll r_e$ and $\alpha \gtrsim 1$, the difference will almost certainly be much less than the uncertainty in r_e from the fitting process itself (see, e.g., Paper III).

The core-Sérsic model in its general form has six free parameters, one more than the Nuker law. However, it is possible that when fitting real galaxy profiles the parameter α , which controls the sharpness of the transition between outer Sérsic and inner power-law regimes, may not be necessary. If a galaxy has a distinct (power-law) core, then the transition to the outer Sérsic profile could, in principle, not be fully resolvable, and might be adequately modeled using $\alpha = \infty$ (i.e., the sharp-transition model, Eqn. 5). The *Nuker law* requires low values of α , for both core *and* power-law galaxies, because this is the only way to create the significant curvature needed to reproduce the observed curvature of galaxy profiles. But since the Sérsic part of our profile already models that curvature, we do not automatically need a low- α transition. There are additionally two mathematical reasons for preferring the sharp-transition model. First, it reduces the number of free parameters in the model to five. Second, a smooth transition (low α) distorts the meaning

⁴In the $\alpha = \infty$ case the definition of b is simpler; see Eq. A12.

⁵This is the version given in Paper I, where r_e was used for what we term r_{es} here.

of the other parameters, so that, for example, the logarithmic slope of the inner profile is *not* equal to γ except at very small radii (as discussed in Section 2).

Thus, we use *both* Eqns. 3 and 5 to model galaxy profiles. Our hope, from the standpoint of simplicity and more transparent meaning for the model parameters, is that the sharp-transition model will be sufficient for core galaxies; as we show in Section 5.3, this appears to be the case.

5. Fits to Galaxy Profiles

5.1. Fitting Techniques and Comparisons with Previous Fits

We fitted various models to the profiles using two standard nonlinear least-squares techniques: the downhill simplex (“amoeba”) method, and the Levenberg-Marquardt method (see, e.g., Press et al. 1992); many of the profiles were also fit using a quasi-Newton algorithm (Kahaner, Moler, & Nash 1989). This went some way towards ensuring that our results were not dependent on the peculiarities of a single method, or its implementation. In general, we found excellent agreement between fits obtained with the three methods. We also tried a variety of starting parameters, to ensure that our fits did not get trapped in local χ^2 minima. Following Byun et al. (1996), we weighted all points equally.

One test of our fitting methods is to see how well we reproduce the original Nuker-law fits of Byun et al. (1996) and Rest et al. (2001), if we restrict the radial range to that of the published PC profiles. In general, we did fairly well at this. There are minor differences between our Nuker-law fits and those of Byun et al. (typically only 10–20% in parameter values) because the latter performed their fits to the equivalent radius ($r_{\text{eq}} = \sqrt{ab}$) profiles, rather than to the major-axis profiles as we do. They also used the (unpublished) cumulative $r \leq 0''.1$ flux as an additional constraint on the fits in some cases.

We found similarly good agreement with the original Rest et al. fits for about two-thirds of the galaxies drawn from their sample; but more significant differences exist for the remainder. There are two probable reasons for this. First, Rest et al. used a somewhat complex scheme of weighting the data points by the errors, while we weight all points equally. Second, their deconvolved profiles are often *not* evenly sampled in logarithmic radius; this can have the effect of giving more weight to points at smaller radii. For example, we get a much closer match to the their Nuker-law fit for NGC 5576 if we fit to $a \leq 5''$ in our combined profile instead of $a \leq 16''$, since there are few data points in their deconvolved profile beyond $a = 5''$ (our combined profiles have had any such gaps filled in with points from the ellipse fits to the mosaic image, in order to produce more evenly sampled profiles). This dependence on the radial weighting is probably a manifestation of the general radial sensitivity of Nuker-law fits (Papers I and III), something supported by the fact that when our fits differ significantly from those of Rest et al., our r_b values are always larger.

5.2. Distinguishing Core from Sérsic Profiles

The Nuker team devised a simple set of criteria for separating core from power-law galaxies, based on fitting profiles with the Nuker law (Lauer et al. 1995; Faber et al. 1997): if the Nuker-law break radius was large enough to be well-resolved ($r_b \geq 0''.16$) and the inner power-law slope was sufficiently flat ($\gamma \leq 0.3$), then the galaxy was considered to have a core; otherwise, it was classed as power-law (or possibly as “intermediate”; e.g., Rest et al. 2001; Ravindranath et al. 2001; Laine et al. 2003).

Our approach is somewhat different: we want to determine when a galaxy profile is best fit by one of two profiles, Sérsic or core-Sérsic, and — something which is in principle a separate issue — whether the galaxy has a core or not. Which model provides a better fit can be determined by comparing reduced χ^2 values. Galaxies which are well fit with the Sérsic profile do not, by our definition, have cores. However, just getting a significantly better fit with the core-Sérsic model does not necessarily indicate a *core*. For example, a bright nuclear disk could add a distinct break to an underlying Sérsic profile; the composite would then be better fit by the core-Sérsic model, even though the overall elliptical/bulge profile was still Sérsic. As suggested in Paper I, *we define a “core” as a downward deviation from the inward extrapolation of the outer (Sérsic) profile*. Examples can be seen in Figures 3 and 4.

After some experimentation, we settled on the following criteria for clearly identifying core galaxies:

1. Qualitative identification of cores: attempting to fit an idealized core galaxy with a Sérsic profile produces a characteristic pattern in the residuals (Figure 3). By fitting all galaxy profiles with the Sérsic model and examining the residuals, we can *qualitatively* identify core galaxies.
2. Significantly better fit with core-Sérsic (CS) than with Sérsic models: $\chi^2_\nu(\text{Sérsic}) > 2 \chi^2_\nu(\text{CS})$ indicates that the core-Sérsic fit is clearly better, while $\chi^2_\nu(\text{Sérsic}) \leq 1.2 \chi^2_\nu(\text{CS})$ indicates the Sérsic profile is good enough. Intermediate ratios are ambiguous cases, which we discuss further below.
3. Potential cores must be both well-resolved and represented by enough data points. Cases where the core-Sérsic break radius is greater than the innermost data point are potentially non-Sérsic profiles, but if the power-law regime is defined by only one or two data points, then its reality is dubious (and the inner slope γ will be poorly defined). Thus, for unambiguous core detection we require $r_b > r_2$, where r_2 is the second innermost data point in the profile.
4. Finally, for a true core profile we require that the power-law slope be consistently $<$ the logarithmic slope of the Sérsic fit inside break radius.⁶

⁶This applies to the fitted data only; as $r \rightarrow 0$, the Sérsic slope $\rightarrow 0$ as well, but this happens well inside the

Non-core galaxies can then be divided into two classes: pure Sérsic profiles, and problematic cases, the latter usually due to a significant extra component such as a bright nuclear disk.

Figures 4 and 5 show the fits for core and Sérsic/ambiguous galaxies, respectively; Table 2 lists the parameters of the fits. The classifications are based on *our* fits, although, as we discuss below, we reproduce the core/power-law classifications of Byun et al. (1996) and Rest et al. (2001) almost perfectly. For each galaxy in the figures we show the best Sérsic and core-Sérsic fits to the entire profile. We also show the best Nuker-law fit *to the inner profile obtained from the PC chip*. We do this because we wish to compare how well a Sérsic or core-Sérsic fit to the *entire* profile manages to reproduce the *inner* profile, where the Nuker law has been used. The relative goodness of the fits is given in Table 2, where we list the reduced chi-square values χ^2_ν for the Sérsic and core-Sérsic fits, and in Table 3, where we give rms residuals for all three types of fit (Sérsic, core-Sérsic, and Nuker-law), evaluated in the inner (PC) region. Again, we do this so we can explicitly compare how well the global Sérsic or core-Sérsic fit does at reproducing the inner (*HST*-resolved) part of the profile.

Table 2. Structural Parameters

Galaxy (1)	n (2)	r_e (3)	I_e (4)	I_b (5)	r_b (6)	γ (7)	α (8)	χ^2_ν (9)	NL-Fit Type (10)	Notes (11)	
Core Galaxies											
N2986	3.29	26.1	20.40	—	—	—	—	0.0353	⊂	1	
	5.28	43.5	—	15.51	0.69	0.25	156.8	0.0108			
	5.28	43.5	—	15.51	0.69	0.25	∞	0.0105			
N3348	3.09	19.8	20.10	—	—	—	—	0.0172	⊂		
	3.86	22.4	—	15.23	0.34	0.14	3.79	0.0017			
	3.81	22.3	—	15.17	0.35	0.16	∞	0.0017			
N4168	2.68	25.9	20.84	—	—	—	—	0.0058	⊂		
	7.47	13.6	—	17.80	3.15	0.00	0.72	0.0012			
	3.12	29.2	—	16.66	0.72	0.22	∞	0.0016			
N4291	3.75	15.7	19.88	—	—	—	—	0.0511	⊂		
	5.58	18.2	—	14.56	0.36	0.11	4.42	0.0072			
	5.44	18.1	—	14.48	0.37	0.14	∞	0.0073			
N5557	3.74	23.3	20.47	—	—	—	—	0.0119)		
	4.63	27.6	—	14.69	0.17	0.09	1.61	0.0019			
	4.37	26.8	—	14.74	0.23	0.23	∞	0.0024			
N5903	2.96	31.2	20.94	—	—	—	—	0.0346	⊂		
	5.39	57.5	—	16.30	0.84	0.11	3.11	0.0058			
	5.09	54.2	—	16.20	0.86	0.15	∞	0.0063			
N5982	3.24	20.5	20.04	—	—	—	—	0.0210	⊂		
	4.20	24.4	—	14.86	0.25	0.05	2.50	0.0012			
	4.06	24.0	—	14.81	0.28	0.11	∞	0.0016			
Possible Core Galaxies											
N3613	3.63	34.2	20.63	—	—	—	—	0.0124	⊂	2	
	3.89	37.1	—	14.70	0.13	0.00	4.61	0.0093			
	3.87	36.9	—	14.71	0.15	0.09	∞	0.0092			
N5077	3.56	21.7	20.34	—	—	—	—	0.0453)		
	3.84	22.4	—	15.03	0.22	0.00	2.37	0.0288			
	3.78	22.3	—	15.21	0.36	0.29	∞	0.0285			
Sérsic Galaxies											
N1426	4.95	35.5	22.15	—	—	—	—	0.0014	\		
	5.33	38.0	—	16.97	1.21	0.81	12.2	0.0011			
	5.27	37.7	—	16.88	1.11	0.81	∞	0.0011			
N1700	5.99	34.4	21.95	—	—	—	—	0.0039	\		
	5.98	34.4	—	13.19	(0.03)	0.00	33.9	0.0042			
	5.98	34.4	—	12.94	(0.02)	0.00	∞	0.0042			
N2634	4.54	18.1	21.10	—	—	—	—	0.0050	\		

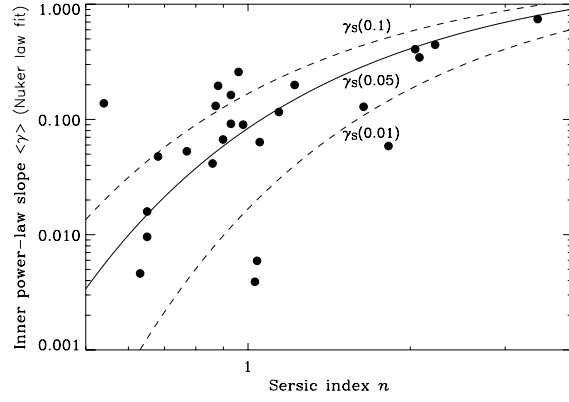


Fig. 2.— Inner logarithmic slope $\langle \gamma \rangle$ (from Nuker-law fits, averaged over $r = 0''.1$ – $0''.5$) versus the Sérsic index n for the dwarf ellipticals of Stiavelli et al. (2001). Also plotted are curves showing the logarithmic slope of the Sérsic function at different fractions of the half-light radius (0.01, 0.05, and $0.1 r_e$), derived using Eq. A15.

5.3. Core Galaxies

Figure 4 shows the profiles and fits for the galaxies we classify as “core” or “possible core.” Notice that the pattern of the Sérsic-fit residuals for these profiles match the pattern in Figure 3: this is excellent (qualitative) evidence for genuine cores in these galaxies. As can be seen, fitting the profiles with the core-Sérsic model largely eliminates these residuals. Table 2 shows, in turn, that the core-Sérsic fits are significantly better, in a more quantitative, statistical sense, than the Sérsic fits for all but the two “possible core” galaxies: reduced chi-square values for Sérsic fits are larger by factors of ~ 3 –15.

In general, we reproduce the core classifications of Rest et al. quite well, while finding that one of their “intermediate” galaxies (NGC 5557) is actually a core galaxy. We classify two galaxies, NGC 3613 and NGC 5077, as “possible core” galaxies. This is because while the core-Sérsic fits are better than the Sérsic fits, they are not significantly so: $\chi^2_\nu(\text{CS}) < 2\chi^2_\nu(\text{Sérsic})$. The patterns of the Sérsic-fit residuals for these galaxies in Figure 4 do suggest possible core profiles, but again this is not strong enough to be convincing. In addition, the break radii from the core-Sérsic fits are near the inner limits of the data; for NGC 3613, $r_b < 0''.16$, the nominal resolution limit of the Nuker team’s core definition. For both galaxies, data at smaller radii are needed to really confirm (or deny) the apparent cores⁷.

Table 2 includes the parameters and χ^2_ν values for fits using both variants of the core-Sérsic model: free α and $\alpha = \infty$ (sharp transition between power-law and Sérsic regimes). By comparing the χ^2_ν values for the core-galaxy and possible-core fits, we can see that in most cases the $\alpha = \text{free}$ fit is only marginally better than the $\alpha = \infty$ fit (see also Column 4 of Table 3). As we suggested in Section 4, the $\alpha = \infty$ model generally provides just as good a fit as the free- α version, while having one less free parameter *and* having parameters values (e.g., γ) which better describe the modeled profile.

There is only one galaxy (NGC 4168) where the free- α fit is significantly different, in terms of parameter values, from the $\alpha = \infty$ fit. We suspect this difference is probably due to the free- α model being better able to fit noise or extra components in the profile, rather than being, e.g., an indication of a core with a genuinely broad transition region. First, there is filamentary dust in the nuclear region (Rest et al. 2001), which produces strong variations in the ellipse fits (Rest et al. and our Figure 10). Second, the $\alpha = \infty$ break radius ($0''.72$, Table 2) matches the apparent break in the profile much better than the free- α value ($3''.15$), as can be seen in Figure 4. Third, the Sérsic index for the $\alpha = \infty$ fit ($n = 3.1$) is more reasonable than the free- α value ($n = 7.5$) for an intermediate-luminosity galaxy (see, e.g., Figure 10 of Graham & Guzmán 2003). Finally, the rms residual values for both fits in the nuclear region (Table 3) are identical, which tells us that the free- α fit does not provide a significantly better description of the core. For these reasons, we do

⁷Rest et al. (2001) noted an edge-on nuclear disk in the inner arc second of NGC 3613, which might explain some of the ambiguity if it is helping to mask a core, or producing a core-like break in the profile.

Table 2—Continued

Galaxy (1)	n (2)	r_e (3)	I_e (4)	I_b (5)	r_b (6)	γ (7)	α (8)	χ^2_ν (9)	NL-Fit Type (10)	Notes (11)
	5.01	18.5	—	17.05	1.51	0.85	8.90	0.0038		
	4.99	18.5	—	17.04	1.52	0.86	∞	0.0038		
N2872	4.56	21.1	20.94	—	—	—	—	0.0048	\	
	4.56	21.1	—	11.54	(0.00)	0.28	17.2	0.0052		
	4.56	21.1	—	11.39	(0.00)	0.30	∞	0.0051		
N3078	4.37	22.9	20.36	—	—	—	—	0.0017	\	
	4.37	22.9	—	13.80	(0.09)	0.29	8.33	0.0018		
	4.37	22.9	—	13.90	(0.10)	0.27	∞	0.0018		
N4458*	10.1	49.0	24.06	—	—	—	—	0.0373	\	3
	10.1	49.1	—	13.65	(0.06)	0.02	15.39	0.0403		
	10.1	49.1	—	14.18	(0.10)	0.30	∞	0.0392		
N4478*	3.11	12.9	19.43	—	—	—	—	0.0484	\	3
	3.11	12.9	—	13.03	(0.00)	0.65	38.00	0.0521		
	2.30	12.5	—	16.29	1.30	0.69	∞	0.0202		
N5017	5.11	11.8	20.44	—	—	—	—	0.0082	\	
	5.11	11.8	—	13.92	(0.10)	0.37	34.5	0.0092		
	5.11	11.8	—	10.00	(0.00)	0.62	∞	0.0092		
N5576	4.74	32.0	20.63	—	—	—	—	0.0084	\	
	4.89	33.7	—	13.15	0.05	0.13	77.0	0.0073		4
	4.89	33.7	—	13.15	0.05	0.13	∞	0.0071		4
N5796	4.79	26.4	21.09	—	—	—	—	0.0189	\	
	4.70	25.6	—	13.70	0.04	0.70	92.6	0.0195		4
	5.25	29.5	—	14.71	0.24	0.51	∞	0.0160		
N5831	4.72	25.5	21.08	—	—	—	—	0.0038	\	
	4.77	25.9	—	13.66	(0.04)	0.30	77.8	0.0038		
	4.72	25.5	—	13.01	(0.01)	0.00	∞	0.0039		
N5845*	2.74	4.57	18.65	—	—	—	—	0.0102	\	3
	2.88	4.36	—	15.79	0.68	0.58	6.74	0.0066		
	2.82	4.44	—	15.64	0.59	0.57	∞	0.0066		

Note. — Structural parameters for fits to the major-axis profiles in our sample. For each galaxy, we list in the first row the best Sérsic fit (n , r_e , I_e) and in the next two rows the best core-Sérsic fits (n , r_e , r_b , I_b , γ , and α ; $\alpha = \infty$ is the sharp-transition version of the core-Sérsic model). When r_b is listed in parentheses, then its value is $<$ the semi-major axis of the second innermost valid data point; consequently, the corresponding power-law region is poorly defined or meaningless. The criteria for assigning galaxies to the different categories (core, possible core, Sérsic) are discussed in the text. Col. (1): Galaxy name. Cols. (2)–(8): Best-fit parameters of the Sérsic and core-Sérsic models (Eqs. 2, 3, 5). The break radius r_b and the effective radius r_e are in arcsec; I_e and I_b are in mag arcsec $^{-2}$ (observed values; no corrections for Galactic extinction or cosmological effects have been made). Col (9): Reduced- χ^2 values for the fits. Col. (10): Original *HST* inner profile classification from Nuker-law fits, from Lauer et al. (1995) or Rest et al. (2001); see Table 1. Col. (11): Notes — 1 = inner parameters (r_b , γ) dubious due to low value of α ; 2 = faint nuclear disk distorts profile; 3 = bright nuclear disk distorts profile; 4 = r_b of indicated fit is between second and third data points of profile.

not think the free- α fit is genuinely better, and we prefer the $\alpha = \infty$ fit for reasons of parsimony.

Finally, how do our core-Sérsic fits compare with Nuker-law fits in terms of reproducing the observed profiles? Table 3 compares rms residuals for the parts of the profile originally extracted from the PC chip of WF/PC1 or WFPC2 and fit with the Nuker law by Byun et al. (1996) and Rest et al. (2001). We remind the reader that the core-Sérsic fit is to the *entire* profile, while the Nuker-law fits are to the PC part of the profile only. Thus, the Nuker-law fit for NGC 3348, for example, is to semi-major axis $a = 0''.02\text{--}14''.5$, while the core-Sérsic fit(s) are to $a = 0''.02\text{--}78''.5$; but the rms residuals are determined for the same $a = 0''.02\text{--}14''.5$ region in both cases.

For the core galaxies, the core-Sérsic fit residuals in the PC region are never more than 20% larger than the Nuker-law residuals; the mean excess is only 3%, and for three of the seven galaxies, the core-Sérsic residuals are equal to or *less than* the Nuker-law residuals. This is rather astonishing, given that the core-Sérsic fit is constrained to fit the profiles out to ~ 5 times further in radius while still having approximately the same number of parameters (exactly the same, in the case of the $\alpha = \infty$ core-Sérsic model). Casual inspection of Figure 4 shows that the Nuker-law fits become much worse than the core-Sérsic fits outside the PC part of the profile, as might be expected. We also note that the *parameter* γ from our $\alpha = \infty$ core-Sérsic fits is usually a closer match to the *observed* slope (γ' , evaluated at $r = 0''.1$, from Rest et al. 2001) than is the Nuker-law parameter γ ; see Table 4.

5.4. Sérsic Galaxies

The remaining twelve galaxies (Figures 5 and 6) are those for which there is no clear evidence for a core: the residuals of the Sérsic fits do not display the characteristic “core pattern” (Figure 3), and the core-Sérsic fits are not significantly better in terms of χ^2_ν . In fact, for seven of these twelve galaxies one or both of the best core-Sérsic (α free or $\alpha = \infty$) fits *reproduces* the best Sérsic fit: the n and r_e parameters are identical, and the core-Sérsic break radius $r_b <$ the innermost data point. Core-Sérsic fits of this nature are clear evidence that these galaxies’ profiles are well described by pure Sérsic profiles. For another four of the galaxies, the n and r_e parameters differ by less than 5% between the core-Sérsic and Sérsic fits, and so the pure Sérsic profile is also preferred for reasons of simplicity.

All twelve of these galaxies were previously classified as power-law galaxies by Byun et al. (1996) or Rest et al. (2001), based on their Nuker-law fits. A comparison of the residuals (Table 3) shows that the Nuker law does fit the inner (PC) profiles slightly better, though, as Figures 5 and 6 show, the Nuker-law residuals are always worse — usually much worse — at larger radii. It is not too surprising that a fit using five parameters (the Nuker law), restricted to the inner $10\text{--}17''$, does better in that region than a fit using only three parameters which also fits the profile out to 3–8 times further in radius. Nonetheless, for six of these galaxies, the (inner) Sérsic-fit rms residuals are < 2 times the Nuker-law residuals, and for only one galaxy are the Sérsic residuals > 3 times

Table 3. Residuals of Fits in the Inner Region of Galaxy Profiles

Galaxy (1)	Profile ranges (2)	Sérsic rms (3)	CS rms (4)	Nuker-law rms (5)	Notes (6)
Core Galaxies					
N2986	0.02–14.4/76.9	0.19	0.054/0.054	0.053	
N3348	0.02–14.5/78.5	0.14	0.040/0.042	0.047	
N4168	0.10–14.7/60.7	0.073	0.037/0.037	0.037	
N4291	0.04–17.4/84.0	0.24	0.050/0.053	0.044	
N5557	0.02–14.6/86.5	0.12	0.041/0.050	0.044	
N5903	0.02–16.2/86.5	0.20	0.073/0.079	0.069	
N5982	0.03–17.0/79.2	0.15	0.030/0.037	0.044	
Possible Core Galaxies					
N3613	0.05–18.4/94.5	0.11	0.068/0.070	0.049	
N5077	0.14–17.1/79.6	0.072	0.045/0.047	0.041	
Sérsic Galaxies					
N1426	0.35–10.2/81.6	0.041	0.030/0.031	0.015	1
N1700	0.13–10.2/62.5	0.061	0.061/0.061	0.028	2
N2634	0.10–13.7/55.5	0.066	0.046/0.046	0.027	
N2872	0.39–14.6/49.3	0.045	0.045/0.045	0.028	2
N3078	0.63–16.7/79.2	0.025	0.025/0.025	0.015	2
N4458	0.18–1.45/68.2	0.16	0.16/0.16	0.045	1,2
N4478	0.02–14.9/70.3	0.23	0.23/0.15	0.11	1,3
N5017	0.33–15.2/55.5	0.080	0.080/0.080	0.027	2
N5576	0.02–16.0/77.5	0.073	0.063/0.064	0.046	
N5796	0.02–12.7/76.9	0.15	0.15/0.15	0.14	3
N5831	0.02–14.9/68.3	0.061	0.057/0.061	0.053	3
N5845	0.02–10.2/39.0	0.097	0.060/0.062	0.064	1

Note. — Comparison of rms residuals for various fits in the inner region (defined as that region fit with the Nuker-law for each galaxy in Byun et al. 1996 or Rest et al. 2001). The Nuker-law rms is from our fit to the corresponding region; the Sérsic and core-Sérsic (CS) rms are from our fits to the *entire* profile, with the residuals calculated in the inner region only. Col. (1): Galaxy name. Col. (2): Fitted regions of profile (semi-major axis, in arc seconds). The first range is the “inner region” (fit with Nuker law), followed by outer limit of the Sérsic and core-Sérsic fits. Col. (3): rms residuals, in magnitudes, of Sérsic fit, calculated in Nuker-law fit region. Col. (4): same as (3), but for the core-Sérsic fits — first number is for free- α version, second is for $\alpha = \infty$. Col. (5): rms residuals of Nuker-law fit. Col. (6) Notes: 1 = nuclear disk; 2 = both core-Sérsic fits reproduce Sérsic fit; 3 $\alpha = \infty$ core-Sérsic fit reproduces Sérsic fit.

the Nuker-law residuals. As we discuss below, the strongest discrepancies are probably due to extra components such as nuclear disks.

There are five power-law galaxies where the Nuker fit is clearly better (in the inner region) — NGC 1426, 2634, 4458, 4478, and 5017. In four of these galaxies (NGC 1426, 4458, 4478, and 5845), there is clear evidence for a luminous nuclear disk (see Figure 7 and the ellipse fits in Appendix B), with the break radius in the Nuker-law fits (and some of the core-Sérsic fits) occurring close to the point of maximum ellipticity associated with the nuclear disks. The distortions created by the nuclear disks in NGC 4458 and NGC 4478 are so strong — producing the largest residuals of any of the galaxies — that we do not consider the Sérsic fits to be reliable. A similarly strong nuclear disk (combined with a dust disk) is found in NGC 5845 (e.g., Quillen, Bowen, & Stritzinger 2000), so the Sérsic fit there may not be reliable either, although the Nuker-law fit is not dramatically better. There is evidence for a slight break in NGC 2634’s surface-brightness profile at $a \sim 2''$, though there is no accompanying signature in the ellipse fits — perhaps a face-on nuclear disk? NGC 5017 is also somewhat mysterious, but the fact that the core-Sérsic fits reproduce the Sérsic fit (Table 2) shows that this is not a core galaxy, and we tentatively include it with the Sérsic galaxies.

We note that the residuals for *all* of the fits to NGC 5796 are large, but this is clearly attributable to the noise in the profile at $a < 0''.2$.

6. Discussion

We conclude that most, if not all, “power-law” ellipticals are probably best understood as having Sérsic profiles — modulo extra components such as nuclear star clusters, nuclear disks, etc. — into the limits of resolution (or limits imposed by dust). As discussed in Section 2, this is consistent with an overall trend for elliptical galaxies: low- and intermediate-luminosity ellipticals have pure Sérsic profiles (plus optional nuclear disks, clusters, and point sources), and distinct cores appear in high-luminosity systems as deviations from the outer Sérsic profile. (Graham & Guzmán 2003 combine measurements for a large set of elliptical galaxies, including dwarf ellipticals, to make this argument in more detail.) Moreover, for power-law galaxies, we get excellent fits using a model with fewer parameters, all of which are physically meaningful (i.e., correlate with other galaxy parameters). These fits work for the *entire* profile, *unlike* the Nuker law, yet are as good a fit in the region where the Nuker law is usually used.

The term “power-law galaxy” is thus somewhat misleading, since it suggests that the nuclear profile is adequately described by a single power-law, which is probably different from the outer profile. While this is an appealingly simple description for modeling purposes, our results strongly suggest that this is not accurate. Instead, elliptical galaxy profiles have logarithmic slopes which continuously decrease as $r \rightarrow 0$. Figure 11 of Lauer et al. (1995), which presents representative examples of “power-law” profiles, supports this argument: even the galaxy which is closest to a perfect power-law, NGC 1700, shows a systematic deviation from a power-law — steeper at larger

radii, shallower at smaller radii — as expected for a Sérsic profile; see Figure 5. (This is not the case for the central cusps of *core* galaxies; see their Figure 7.)

The “intermediate” galaxies reported by Rest et al. (2001) and Ravindranath et al. (2001) are probably a consequence of Nuker-law fits applied to this overall elliptical-galaxy trend. Lower-luminosity “intermediate” galaxies are most likely Sérsic galaxies with low values of n (and hence $\langle \gamma \rangle$ in the range 0.3–0.5; see Fig. 2). At higher luminosities, core galaxies can appear to have $\gamma > 0.3$ if the core is not adequately resolved (either due to distance or to inner truncation of the profile by, e.g., dust). (We *do* classify two galaxies in our sample as “possible core” galaxies, but these are clearly cases of inadequate resolution.)

Although we have not yet attempted to model the complete profiles of *bulges*, it is reasonable to extend our results to them. Balcells et al. (2003) have already done this for a sample of early-type bulges in the near-IR, using NICMOS data in conjunction with ground-based imaging. They find that the complete bulge profiles, after accounting for the presence of the outer disk, can be well modeled by Sérsic profiles, plus optional nuclear components (corresponding to, e.g., nuclear star clusters or point sources). This is in excellent agreement with our hypothesis that the profiles of lower-luminosity ellipticals and bulges are fundamentally Sérsic profiles, and promises to resolve a number of ambiguities and “dichotomies” reported in the literature. For example, Carollo et al. (1997) and Seigar et al. (2002) argue for a dichotomy between $R^{1/4}$ and exponential bulges, with the latter having low γ in contrast to the high γ of $R^{1/4}$ bulges and moderate-luminosity ellipticals. This is naturally explained if most bulges actually have Sérsic profiles (as is well supported by a number of studies) *and* if these Sérsic profiles extend into the nuclear region. The division between $R^{1/4}$ (Sérsic index $n = 4$) and exponential ($n = 1$) bulges is probably an artificial one, given that bulges in reality show a range of values of n . But as Paper I shows, bulges with larger n will have higher values of γ than bulges with low n . Thus, “ $R^{1/4}$ ” bulges (higher n) will exhibit larger values of γ than “exponential” (lower n) bulges. Since bulge n decreases along the Hubble sequence, the trend of decreasing γ with Hubble type noted by Seigar et al. (2002, their Fig. 3) follows as well.

In retrospect, we can see that most of the early *HST* studies of galaxy centers, and some of the more recent ones (e.g., Rest et al. 2001; Ravindranath et al. 2001), have focused on relatively high-luminosity systems. These samples thus included a mix of Sérsic galaxies with high n values and genuine core galaxies, making a distinction between core and “power-law” galaxies based purely on γ feasible. More recent studies aimed at low-luminosity systems (e.g., Carollo & Stiavelli 1998; Stiavelli et al. 2001; Seigar et al. 2002) have since uncovered evidence for the low- n –low- γ , high- n –high- γ trend that pure Sérsic profiles generate, and thus show that discriminating core galaxies purely by γ is problematic at best.

6.1. Core Identifications and Core Parameters

We find that most of the previously identified “core” galaxies in our sample *do* have distinct cores with shallow, power-law cusps. These cores stand out as downward deviations from the outer Sérsic profiles. Fitting with the core-Sérsic model provides a more natural, less ambiguous definition for “true” cores, without the possibility of misclassifying low- n Sérsic profiles as cores. We are also able to re-classify one of the “intermediate” galaxies (NGC 5557) of Rest et al. (2001) as a core galaxy. The two ambiguous galaxies — NGC 3613 and NGC 5077 — are simply cases where the apparent break radius is very close to the inner limits of the data. For NGC 3613, this is because the apparent core is close to the resolution limit (in fact, r_b from the core-Sérsic fits is $< 0''.16$ and thus smaller than the suggested resolution-based limit of Faber et al. 1997). For NGC 5077, on the other hand, Rest et al. (2001) clipped their data at $r = 0''.1$ because of an apparent nuclear excess at smaller radii. A future fit including data at smaller radii and using an extra nuclear component to account for this excess, may help determine if NGC 5077 truly possesses a core.

While our overall agreement with the core/non-core classifications of Lauer et al. (1995) and Rest et al. (2001) is quite good for the galaxies we analyze, *we find that Nuker-law fits systematically overestimate the size of the cores*: our break radii are ~ 1.5 – 4.5 times smaller in size than the break radii from the published Nuker-law fits. Consequently, μ_b values are brighter as well. We also find consistently higher values of γ , though the difference is not as dramatic (see Table 4 and Figure 8). This is in excellent agreement with the arguments of Papers I and III: *all* Nuker-law parameters are sensitive to the radial size of the region where the fit is made. All parameters of the Nuker model, including γ and r_b , must be adjusted in order to fit both the core *and* the (non-power-law) part of the profile outside, with its intrinsic (Sérsic) curvature. Table 4 shows that, on average, the core-Sérsic values of γ match the *observed* core slope γ' (as determined by Rest et al. (2001)) better than the Nuker-law values do.

The currently favored theory for core formation is the ejection of core stars by 3-body encounters with a decaying black hole binary formed following a merger of two galaxies with central supermassive black holes. Various calculations (Ebisuzaki, Makino, & Okamura 1991; Quinlan & Hernquist 1997; Milosavljević & Merritt 2001) have estimated the stellar mass ejected during this process (M_{ej}), and generally find it to be $\sim M_{\text{BH}}$, where M_{BH} is the mass of the resulting central black hole formed by the (assumed) coalescence of the binary. However, attempts to test these predictions by estimating M_{ej} from observed cores and comparing it with various estimates of M_{BH} consistently produce values of $M_{\text{ej}} > M_{\text{BH}}$. Faber et al. (1997) found $M_{\text{ej}} = 3.5$ – $6.4 M_{\text{BH}}$; using more accurate estimates of M_{BH} , Milosavljević & Merritt (2001) found $M_{\text{ej}} \approx 1$ – $20 M_{\text{BH}}$. Ravindranath, Ho, & Filippenko (2002) used the prescription for M_{ej} of Milosavljević & Merritt and a much larger data set; they found $M_{\text{ej}} \approx 2$ – $20 M_{\text{BH}}$ at the low-mass end ($M_{\text{BH}} \sim 10^8 M_{\odot}$), while at the high-mass end ($M_{\text{BH}} \sim 10^9 M_{\odot}$) $M_{\text{ej}} \approx 6$ – $25 M_{\text{BH}}$. Even considering only the galaxies with *measured* M_{BH} , $M_{\text{ej}}/M_{\text{BH}} \approx 4$ – 13 . Milosavljević & Merritt pointed out that the *total* ejected mass should increase with the number of mergers, but the observed ratios still seem high, particularly at the low-mass end, where there have presumably been fewer mergers.

All of the studies cited above used parameters from Nuker-law fits to estimate M_{ej} . Since the estimated M_{ej} scales with r_b — in the parameterization introduced by Milosavljević & Merritt (2001) and used by Ravindranath et al. (2002), $M_{\text{ej}} \propto r_b$ — overestimating r_b will naturally overestimate M_{ej} . Thus at least some of the discrepancy between observed and predicted $M_{\text{ej}}/M_{\text{BH}}$ is probably due to the tendency of Nuker-law fits to overestimate r_b , as we have found. Assuming that the core radii from core-Sérsic fits are typically ~ 2 – 4 times smaller than the Nuker-law values, as is the case for our sample, $M_{\text{ej}}/M_{\text{BH}}$ values should go down by comparable factors, which would put them in better agreement with the theoretical predictions.

One of our core galaxies (NGC 4291) was noted by Ravindranath et al. (2001) for possibly having an isothermal core (with $\gamma = 0$), on the basis of their Nuker-law fits to a NICMOS image. The Nuker-law fit in Rest et al. (2001) to the WFPC2 profile also has $\gamma = 0.0$, which might seem to strengthen the case for an isothermal core. However, we find $\gamma = 0.14$ from our core-Sérsic fit, which agrees very well with $\gamma' = 0.13$ determined by Rest et al. So the core of NGC 4291 is probably *not* isothermal.

In Figure 9 we show the relation between the core and the global properties of the galaxies in our sample. We also indicate the upper limits on possible core radii for the Sérsic galaxies, based on the radii of the innermost valid data. For those galaxies where a clear core has been measured, we find that the relation between the break radius and the effective radius is approximately given by $r_b = 0.014r_e$. This is a factor of two smaller than the relation found by Faber et al. (1997), consistent with our finding that fitting with the Nuker law tends to overestimate core sizes.

There is a suggestion of a weak trend of r_b increasing with galaxy luminosity, which would be in agreement with what Faber et al. found (see also Laine et al. 2003), but for our sample this “trend” is anchored by only two points, so it is dubious. Unfortunately, the narrow magnitude range spanned by the core galaxies in our sample ($\lesssim 1.5$ mag) precludes a proper test of the magnitude- r_b relation reported Faber et al., which is based on galaxies spanning $\gtrsim 3$ mag (and the composite trend in Fig. 9 of Laine et al. spans almost 5 magnitudes). There is no clear magnitude-related trend in the *ratio* of our r_b measurements to the Nuker-law measurements, which suggests that the magnitude- r_b trend may be unaffected by changes in r_b , except possibly in the scatter. However, a proper evaluation of how the magnitude- r_b relation is affected by better measurements of r_b must await core-Sérsic fits to a larger sample of core galaxies. There is *no* evidence for a relationship between n and r_b ; this may be partly due to large uncertainties in n (Caon et al. 1993 found typical errors of $\sim 25\%$ when fitting Sérsic profiles). Finally, we find *no* clear correlation between γ and the global properties of the core galaxies analyzed. This is agreement with what previous studies have found for core galaxies (e.g., Rest et al. 2001, Figure 7; Ravindranath et al. 2001, Figure 3; Laine et al. 2003, Figure 6; and the core galaxies in Figure 1 of this paper).

6.2. Hidden Cores and the Core-Galaxy Fraction

An interesting point is to consider how well-resolved the underlying profiles of the various galaxies actually are. In several cases, Byun et al. (1996) and Rest et al. (2001) excluded points at small radii from their fits, usually due to the presence of significant nuclear dust or a distinct nuclear component (e.g., a nuclear point source). Thus, not all of the profiles take full advantage of *HST* resolution. While the nuclear components may include cases of nuclear star clusters, which make discussions of the underlying stellar profile ambiguous, the presence of dust means that some “power-law” (i.e., Sérsic-profile) galaxies could have hidden cores.

If we divide the sample into two groups — galaxies where the innermost valid data point is at $r < 15$ pc (spatially well resolved centers); and galaxies where the innermost valid point is at $r > 15$ pc (less well-resolved centers) — we find that the *less* resolved galaxies are almost all⁸ well fit using just the Sérsic model. This suggests that at least some of the Sérsic galaxies could have “hidden” cores. This is not a new argument, obviously, as many authors have pointed out that “power-law” galaxies could include unresolved cores — but it is interesting to consider how *few* of the Sérsic galaxies in our sample can really be declared free of *HST*-resolvable cores. Of the 21 galaxies, seven clearly have cores, two have possible cores (NGC 3613 and NGC 5077, see Section 6.1), and only five (NGC 4478, NGC 5576, NGC 5796, NGC 5831, and NGC 5845) are clearly free of significant ($r_b > 5$ pc) cores.

So in the limited range of absolute magnitude spanned by our full sample ($-18.3 \gtrsim M_B \gtrsim -21.4$), 33% of the galaxies have unambiguous, *HST*-resolved cores; but this is clearly a lower limit. The core fraction rises to 43% if we include the two possible cases, and in principle could be as high as 76%. It is also interesting to note that we can see in the absolute magnitudes a hint of the well-known dichotomy between core and non-core galaxies (see, e.g., the discussion in Rest et al. 2001), even in our limited sample. This can be seen in Figure 9, where the five *fully resolved* Sérsic galaxies tend to be fainter than the core galaxies; a Kolmogorov-Smirnov test gives a 95% probability that the two groups of galaxies come from different parent luminosity distributions.

7. Summary

We have successfully fit the complete surface-brightness profiles of 19 out of 21 elliptical galaxies, from the *HST*-resolved central regions ($r \sim 0''.02$) out to \sim twice the half-light radius, using either: a) a pure Sérsic profile; or b) a “core-Sérsic” model consisting of an outer Sérsic profile joined to an inner power-law core. The former fits correspond to so-called “power-law” galaxies, which are perhaps better described as “Sérsic galaxies,” and the latter correspond to core galaxies.

The combined use of these two models lets us address the following questions:

⁸The exceptions are NGC 4168 (core) and NGC 5077 (possible core).

1. *How can we relate the central, HST-resolved part of the galaxies’ surface-brightness profiles to the outer regions?* We show that most power-law ellipticals are well described at all radii by the simple Sérsic law (modulo any nuclear disks, etc.). On the other hand, core galaxies are extremely well fit with the core-Sérsic model. We find little need for a significant transition region between the outer (Sérsic) part of the core-Sérsic profile and the (power-law) core; any such transition region is small compared to the size of the core.
2. *Is there a dichotomy in nuclear profiles between low- and high-luminosity bulges and ellipticals?* Some recent *HST* studies have suggested that the apparent trend seen in intermediate- and high-luminosity bulges and ellipticals — cores with shallow logarithmic slopes in high-luminosity systems, steeper nuclear slopes in lower-luminosity (“power-law”) systems — breaks down at lower luminosities, because fainter bulges and dwarf ellipticals have shallow nuclear slopes. We show that the power-law galaxies in our sample have Sérsic profiles that extend into the limits of *HST* resolution, with $n \sim 4\text{--}6$; this naturally explains the steep nuclear slopes previously reported. When combined with the well-known correlation between n and luminosity, we can see that (as argued by Graham & Guzmán 2003) the general trend is most likely one of pure Sérsic profiles (plus possible extra components such as nuclear star clusters and disks), extending from low-luminosity systems with low- n Sérsic profiles — and thus shallow nuclear slopes — to high-luminosity systems with high- n profiles and steeper nuclear slopes. Only the high-luminosity *core* galaxies break the trend, due to the existence of the cores themselves.
3. *How can we unambiguously identify cores in galaxy profiles?* As we demonstrate, the traditional definition of cores using parameters from Nuker-law fits to galaxy profiles ($r_b \geq 0''.16$ and $\gamma < 0.3$) leads to the real possibility of misclassifying galaxies with sufficiently shallow slopes (for example, exponential profiles) as core galaxies. *We define core galaxies as those possessing a well-resolved downward deviation from the inward extrapolation of the outer (Sérsic) profile.* This definition recovers previous core definitions for the high-luminosity ellipticals in our sample, but is immune to the danger of identifying exponential-like profiles as having cores.
4. *How can we more accurately determine the structural properties of cores?* As demonstrated in Paper I, the Nuker law requires a broad, smooth transition (low values of α) between its two power-law regimes in order to fit the inner profiles of core and power-law galaxies, because this is the only way to reproduce the observed curvature of actual galaxy profiles. We find that this causes the core-size measurements (i.e., the break radius) to be overestimated by factors of 1.5–4.5 in comparison to the values derived by using the core-Sérsic model, which directly accounts for the intrinsic curvature of galaxy profiles. We also find that the logarithmic slope γ of the observed core is more accurately recovered with the core-Sérsic model. Using the smaller values we find, especially for r_b , should bring estimates of the ejected stellar mass due to core formation more in line with theoretical predictions.

We thank Linda S. Sparke for useful discussions. This research is based on observations made with the NASA/ESA Hubble Space Telescope, obtained from the data archive at the Space Telescope Institute. STScI is operated by the association of Universities for Research in Astronomy, Inc. under the NASA contract NAS 5-26555.

This research also made use of the Lyon-Meudon Extragalactic Database (LEDA; <http://leda.univ-lyon1.fr>), and the NASA/IPAC Extragalactic Database (NED), which is operated by the Jet Propulsion Laboratory, California Institute of Technology, under contract with the National Aeronautics and Space Administration.

REFERENCES

- Andredakis, Y., Peletier, R., Balcells, M., 1995, MNRAS, 275, 874
- Balcells, M., Graham, A. W., Domínguez-Palmero, L., & Peletier, R. F. 2003, ApJ, 582, L79
- Binggeli, B., & Jerjen, H. 1998, A&A, 333, 17
- Byun, Y.-I., et al. 1996, AJ, 111, 1889
- Caldwell, N. 1999, AJ, 118, 1230
- Caon, N., Capaccioli, M., & D’Onofrio, M. 1993, MNRAS, 265, 1013
- Capaccioli, M. 1987, in Structure and Dynamics of Elliptical Galaxies, IAU Symp. 127, ed. T. de Zeeuw (Dordrecht: Reidel), 47
- Carollo, C. M., Franx, M., Illingworth, G. D., & Forbes, D. A. 1997, ApJ, 481, 710
- Carollo, C. M., & Stiavelli, M. 1998, AJ, 115, 2306
- Cellone, S. A., Forte, J. C., & Geisler, D. 1994, ApJS, 93, 397
- Crane, P., et al. 1993, AJ, 106
- Davies, J. I., Phillipps, S., Cawson, M. G. M., Disney, M. J., & Kibblewhite, E. J. 1988, MNRAS, 232, 239
- de Vaucouleurs, G. 1959, Hand. Phys., Vol. 53, 311
- de Vaucouleurs, G., de Vaucouleurs, A., Corwin, H. G., Buta, R. J., Paturel, G., & Fouqué, P. 1991, Third Reference Catalogue of Bright Galaxies (New York: Springer-Verlag) (RC3)
- Durrell, P. R. 1997, AJ, 113, 531
- Ebisuzaki, T., Makino, J., & Okamura, S. K. 1991, Nature, 354, 212
- Erwin, P., Sparke, L. S. 2003, ApJS, 146, 299

- Erwin, P., Caon, N., & Graham, A. W. 2003, in *Carnegie Observatories Astrophysics Series, Vol. 1: Coevolution of Black Holes and Galaxies*, ed. L. C. Ho (Pasadena: Carnegie Observatories, <http://www.ociw.edu/ociw/symposia/series/symposium1/proceedings.html>)
- Erwin, P., Caon, N., & Graham, A. W. 2004a, in prep
- Erwin, P., Graham, A. W., & Trujillo, I. 2004b, in prep (Paper III)
- Faber, S. M., et al. 1997, *AJ*, 114, 1771
- Ferrarese, L., van den Bosch, F. C., Ford, H. C., Jaffe, W., & O’Connell, R. W., 1994, *AJ*, 108, 1598
- Freedman, W., et al. 2001, *ApJ*, 553, 47
- Gebhardt, K., et al. 1996, *AJ*, 112, 105
- Geha, M., Guhathakurta, P., & van der Marel, R. P. 2002, *AJ*, 124, 3073
- Graham, A. W., 2001, *AJ*, 121, 820
- Graham, A. W., 2002, *MNRAS*, 334, 859
- Graham, A. W., & Guzmán, R. 2003, *AJ*, 125, 2936
- Graham, A., Lauer, T. R., Colless, M., & Postman, M. 1996, *ApJ*, 465, 534
- Graham, A. W., Trujillo, I., & Caon, N. 2001a, *AJ*, 122, 1707
- Graham, A. W., Erwin, P., Caon, N., & Trujillo, I. 2001b, *ApJ*, 563, L11
- Graham, A. W., Erwin, P., Trujillo, I., & Asensio, A. 2003a, *AJ*, 125, 2951 (Paper I)
- Graham, A. W., Erwin, P., Caon, N., & Trujillo, I. 2003b, in *Galaxy Evolution: Theory and Observations*, *RevMexAA (SC)*, eds. V. Avila-Reese, C. Firmani, C.S. Frenk, & C. Allen, 196
- Graham, A. W., Erwin, P., Trujillo, I., & Asensio, A. 2003c, in *Carnegie Observatories Astrophysics Series, Vol. 1: Coevolution of Black Holes and Galaxies*, ed. L. C. Ho (Pasadena: Carnegie Observatories, <http://www.ociw.edu/ociw/symposia/series/symposium1/proceedings.html>)
- Grillmair, C. J., et al. 1994, *AJ*, 108, 102
- Jaffe, W., Ford, H. C., O’Connell, R. W., van den Bosch, F. C., & Ferrarese, L. 1994, *AJ*, 108, 1567
- Jerjen, H., Binggeli, B., & Freeman, K. C. 2000, *AJ*, 119, 593
- Kent, S. M. 1985, *ApJS*, 59, 115

- Kahaner, D., Moler, C., & Nash, S. 1989, *Numerical Methods and Software* (Englewood Cliffs, NJ: Prentice Hall)
- Khosroshahi, H. G., Wadadekar, Y., Kembhavi, A., 2000, *ApJ*, 533, 162
- Kormendy, J., 1985, *ApJ*, 292, L9
- Kormendy, J., Dressler, A., Byun, Y. I., Faber, S. M., Grillmair, C., Lauer, T. R., Richstone, D., Tremaine, S. 1994, in *ESO/OHP Workshop on Dwarf Galaxies*, ed. G. Meylan & P. Prugniel (Garching: ESO), 147
- Lauer, T. R., 1985, *ApJ*, 292, 104
- Lauer, T. R., et al. 1995, *AJ*, 110, 2622
- Laine, S., van der Marel, R. P., Lauer, T. R., Postman, M., O’Dea, C. P., & Owen, F. Z., 2003, *AJ*, 125, 478
- MacArthur, L. A., Courteau, S., & Holtzman, J. A. 2003, *ApJ*, 582, 689
- McElroy, D. B., 1995, *ApJS*, 100, 105
- Milosavljević, M., & Merritt, D. M. 2001, *ApJ*, 563, 34
- Milosavljević, M., Merritt, D. M., Rest, A., & van den Bosch, F. C. 2002, *MNRAS*, 331, L51
- Möllenhoff, C., & Heidt, J. 2001, *A&A*, 368, 16
- Nieto, J.-L., Bender, R., Poulain, P., & Surma, P. 1992, *A&A*, 257, 92
- Paturel, G., et al. 1997, *A&AS*, 124, 109
- Quillen, A. C., Bower, G. A., & Stritzinger, M. 2000, *ApJS*, 128, 85
- Press, W. H., Teukolsky, S. A., Vetterling, W. T., & Flannery, B. P. 1992, *Numerical Recipes in C*, 2nd ed. (Cambridge: Cambridge U. Press)
- Quinlan, G. D., & Hernquist, L. 1997, *NewA*, 2, 533
- Ravindranath, S., Ho, L. C., Peng, C. Y., Filippenko, A. V., & Sargent, W. L. W. 2001, *AJ*, 122, 653
- Ravindranath, S., Ho, L. C., & Filippenko, A. V. 2002, *ApJ*, 566, 801
- Rest, A., van den Bosch, F. C., Jaffe, W., Tran, H., Tsvetanov, Z., Ford, H. C., Davies, J., & Schafer, J. 2001, *AJ*, 121, 2431
- Rix, H.-W., Carollo, C. M., & Freeman, K. 1999, *ApJ*, 513, L25

- Seigar, M. S., & James, P. A. 1998, MNRAS, 299, 672
- Seigar, M., Carollo, C. M., Stiavelli, M., de Zeeuw, P. T., & Dejonghe, H. 2002, AJ, 123, 184
- Sérsic, J.-L., 1968, Atlas de Galaxias Australes (Córdoba: Obs. Astron.)
- Stiavelli, M., Miller, B. W., Ferguson, H. C., Mack, J., Whitmore, B. C., & Lotz, J. M. 2001, AJ, 121, 1385
- Tonry, J. L., Dressler, A., Blakeslee, J. P., Ajhar, E. A., Fletcher, A. B., Luppino, G. A., Metzger, M. R., & Moore, C. B. 2001, ApJ, 546, 681
- Young, C. K., & Currie, M. J. 1994, MNRAS, 268, L11

Table 4. Comparison of Core-Sérsic and Nuker Parameters for Cores

Galaxy (1)	I_b (CS) (2)	r_b (CS) (3)	γ (CS) (4)	I_b (Nuk) (5)	r_b (Nuk) (6)	γ (Nuk) (7)	γ' (8)
N2986	15.5	0.69/97	0.25	16.1	1.24/174	0.18	0.20
N3348	15.2	0.35/70	0.16	16.0	0.99/198	0.09	0.18
N3613	14.7	0.15/21	0.09	15.1	0.34/48	0.04	0.17
N4168	16.7	0.72/108	0.22	17.5	2.02/303	0.17	0.19
N4291	14.5	0.37/47	0.14	15.1	0.60/76	0.00	0.13
N5077	15.2	0.36/62	0.29	16.5	1.61/279	0.23	0.30
N5557	14.7	0.23/51	0.23	16.2	1.21/269	0.14	0.33
N5903	16.2	0.86/141	0.15	16.8	1.59/262	0.13	0.14
N5982	14.8	0.28/57	0.11	15.6	0.74/151	0.00	0.18

Note. — Comparison of core parameters obtained from core-Sérsic (CS) and Nuker-law (Nuk) fits to the core galaxies. The break radii r_b are in arc seconds/parsecs; R -band surface brightness at the break radius is in mag arcsec⁻². We use the $\alpha = \infty$ (sharp-transition) version of the core-Sérsic model for the CS values; the Nuker-law values and the slope at $r = 0.1''$ (γ') are taken from the original fits in Rest et al. (2001).

A. Some Useful Mathematical Expressions Related to the Core-Sérsic Model

A.1. The Relation Between Core-Sérsic and Sérsic Effective Radii

In this section we want to prove the following identity:

$$b_n \left(\frac{1}{r_{es}} \right)^{1/n} = b \left(\frac{1}{r_e} \right)^{1/n}, \quad (\text{A1})$$

where r_{es} is the effective radius of the Sérsic part of the core-Sérsic model, r_e is the effective radius of the global core-Sérsic model, and b_n and b are the quantities introduced in order to give to r_e in the Sérsic and core-Sérsic model, respectively, the meaning of effective radius.

Demonstration: Although the above relation can be proved for smooth transitions between the Sérsic regime and the power-law regime (i.e., α small), we will only show the demonstration for the sharpest transition case ($\alpha \rightarrow \infty$). The Sérsic part of the core-Sérsic model is described using the following law:

$$I(r) = I(0) \exp[-b(r/r_e)^{1/n}], \quad (\text{A2})$$

with

$$I(0) = I_b \exp[b(r_b/r_e)^{1/n}]. \quad (\text{A3})$$

The integrated luminosity out to a given radius for this model is given by:

$$L(r) = \frac{2\pi n}{b^{2n}} r_e^2 I(0) \gamma(2n, b(r/r_e)^{1/n}), \quad (\text{A4})$$

with $\gamma(a, x)$ being the incomplete gamma function. We can now determine the effective radius r_{es} for Eqn. A2 using the effective radius equation:

$$2 L(r_{es}) = L(\infty), \quad (\text{A5})$$

with $L(\infty)$ being the total luminosity. For Eqn. A2, the effective radius equation becomes:

$$2 \gamma(2n, b(r_{es}/r_e)^{1/n}) = \Gamma(2n), \quad (\text{A6})$$

where $\Gamma(a)$ is the complete gamma function. On the other hand, if we have a pure Sérsic law described by the index n the above equation is written as:

$$2 \gamma(2n, b_n) = \Gamma(2n). \quad (\text{A7})$$

It follows immediately that:

$$b_n = b(r_{es}/r_e)^{1/n}, \quad (\text{A8})$$

or, equivalently,

$$b_n (1/r_{es})^{1/n} = b (1/r_e)^{1/n}, \quad (\text{A9})$$

as we wanted to show.

A.2. The Evaluation of b for the Core-Sérsic Model

The quantity b is used in the Sérsic and core-Sérsic models in order to give r_e the meaning of effective radius. In order to evaluate b , it is thus necessary to solve the implicit equation $2L(r_e) = L_T$. For the Sérsic profile ($b = b_n$), as is known, this produces Eqn. A7, given above. For the core-Sérsic model, b is a function of the various parameters (α , γ , r_b , and r_e) in the core-Sérsic model, and can be determined by solving the following relation:

$$2 \int_{b(r_b/r_e)^{1/n}}^{b(1/r_e)^{1/n}(r_b^\alpha + r_e^\alpha)^{1/(n\alpha)}} e^{-x} x^{n(\gamma+\alpha)-1} (x^{n\alpha} - (b^n r_b/r_e)^\alpha)^{(2-\gamma-\alpha)/\alpha} dx = \int_{b(r_b/r_e)^{1/n}}^{+\infty} e^{-x} x^{n(\gamma+\alpha)-1} (x^{n\alpha} - (b^n r_b/r_e)^\alpha)^{(2-\gamma-\alpha)/\alpha} dx. \quad (\text{A10})$$

This assumes that $\alpha > 0$. As $r_b \rightarrow 0$, we recover the Sérsic expression. In the particular case $\alpha \rightarrow \infty$ (sharp transition between inner power-law and outer Sérsic regimes), the equation simplifies to

$$\frac{1}{2-\gamma} \left(\frac{r_b}{r_e} \right)^2 = \frac{n}{b^{2n}} e^{b(r_b/r_e)^{1/n}} \left\{ \Gamma(2n) + \gamma(2n, b(r_b/r_e)^{1/n}) - 2\gamma(2n, b) \right\}. \quad (\text{A11})$$

In practice, as long as $r_b \ll r_e$ and $\gamma < 1$, the above equation can be simplified even more:

$$\Gamma(2n) + \gamma(2n, b(r_b/r_e)^{1/n}) \approx 2\gamma(2n, b). \quad (\text{A12})$$

A.3. Local Logarithmic Slope γ'

Rest et al. (2001) introduced γ' as a measure of the (logarithmic) gradient of the luminosity profile at some specific radius r' :

$$\gamma' \equiv - \left[\frac{d \log I}{d \log r} \right]_{r'}. \quad (\text{A13})$$

For the Nuker law, γ' is (e.g., Rest et al. 2001, Eqn. 8):

$$\gamma' = \frac{\gamma + \beta(r'/r_b)^\alpha}{1 + (r'/r_b)^\alpha}. \quad (\text{A14})$$

As Rest et al. noted, this is a more accurate description of the local logarithmic slope than the Nuker-law parameter γ when the transition between the two power-law regimes is soft (i.e, small α). For the Sérsic profile we have:

$$\gamma' = \frac{b}{n} \left(\frac{r'}{r_e} \right)^{1/n}. \quad (\text{A15})$$

Finally, for the core-Sérsic model:

$$\gamma' = \frac{b}{n} \left(\frac{1}{r_e} \right)^{1/n} r'^\alpha (r'^\alpha + r_b^\alpha)^{1/(n\alpha)-1} + \frac{\gamma(r_b/r')^\alpha}{1 + (r_b/r')^\alpha}. \quad (\text{A16})$$

As $r_b \rightarrow 0$, we recover the Sérsic expression. As $\alpha \rightarrow \infty$, γ' is described by the Sérsic value outside r_b and is $= \gamma$ inside.

A.4. Total Luminosity

We assume the object is circular. If the galaxy is elliptical the following expressions must be multiplied by b/a , where a and b are semi-major and semi-minor axes, respectively. The total luminosity is defined as:

$$L_T = \int_0^{2\pi} \int_0^{+\infty} I(r) r dr d\theta. \quad (\text{A17})$$

For a Sérsic profile the total luminosity is then

$$L_T = \frac{2\pi n}{b^{2n}} \Gamma(2n) I(0) r_e^2, \quad (\text{A18})$$

while for the core-Sérsic model it is

$$L_T = 2\pi I' n \left(\frac{r_e}{b^n} \right)^2 \int_{b(r_b/r_e)^{1/n}}^{+\infty} e^{-x} x^{n(\gamma+\alpha)-1} (x^{n\alpha} - (b^n r_b/r_e)^\alpha)^{(2-\gamma-\alpha)/\alpha} dx. \quad (\text{A19})$$

This expression is valid for $\alpha > 0$. As $r_b \rightarrow 0$, we recover the Sérsic expression. In the particular case $\alpha \rightarrow \infty$, this expression becomes:

$$L_T = 2\pi I_b \left\{ \frac{r_b^2}{2-\gamma} + e^{b(r_b/r_e)^{1/n}} n \frac{r_e^2}{b^{2n}} \left[\Gamma(2n) - \gamma(2n, b(r_b/r_e)^{1/n}) \right] \right\}. \quad (\text{A20})$$

B. Contour Maps and Ellipse Fits

In Figure 10 we display the isophotal contour maps and ellipse fits for the WFPC2 mosaics of each of the galaxies we analyzed. Details of the data reduction can be found in Section 3.2.

C. Galaxies Rejected as Probable S0

The following galaxies met our selection criteria for size and for the existence of WFPC2 archival images in the appropriate filters, but were judged to have significant disks and thus be possible S0 galaxies, despite their formal classification as ellipticals. We err on the conservative side by considering the presence of bars and rings to be evidence for an S0 galaxy; evidence for a bar includes the appearance of the isophotes, peaks in ellipticity and accompanying position-angle twists in the ellipse fits, and typical bar appearance in unsharp masks (see, e.g., Erwin & Sparke 2003). We also use evidence from our attempts to fit the extra-nuclear ($r > 1''$) light profiles (derived from the mosaic images) with both pure Sérsic and disk + bulge models: i.e., there are some galaxies for which Sérsic + exponential is clearly a better fit than pure Sérsic.

NGC 596: Source: Lauer et al. (1995). Nieto et al. (1992) argued that this was actually an SB0 galaxy; Faber et al. (1997) also note that this galaxy has “an S0-like outer envelope.” Our fits to the light profile also suggest a disk + bulge morphology.

NGC 2592: Source: Rest et al. (2001). Kinematic evidence from Rix, Carollo, & Freeman (1998) strongly suggests this is an S0 galaxy; in addition, there is evidence for a bar in the PC isophotes and unsharp masks.

NGC 2699: Source: Rest et al. (2001). Kinematic evidence from Rix et al. (1998) strongly suggests this is an S0 galaxy; in addition, there is clear evidence of a bar in the PC image (Rest et al. 2001 pointed to this galaxy as a providing a good example of a misaligned inner structure, e.g., a bar).

NGC 2778: Source: Rest et al. (2001). Kinematic evidence from Rix et al. (1998) strongly suggests this is an S0 galaxy; in addition, there is good evidence for a bar in the PC image. Analysis of the light profile in Kent (1985) and Erwin et al. (2004a) also supports an S0 (i.e., bulge + outer disk) interpretation.

NGC 3608: Source: Lauer et al. (1995). The light profile is significantly better fit with a disk + bulge model than by a pure Sérsic model; see Erwin et al. (2004a).

NGC 4121: Source: Rest et al. (2001). There is clear evidence for a bar in the PC image (“misaligned inner structure” in Rest et al.), and the extra-nuclear light profile is much better fit with a composite (bulge + disk) model than by a single Sérsic component.

NGC 4564: Source: Rest et al. (2001). Unsharp masking of the PC image indicates that the elliptical feature dominating the isophotes is a stellar ring, which we judge to be a signature of a significant disk; there is some evidence for a nuclear bar as well. Analysis of the light profile in Erwin et al. (2004a) also supports an S0 (i.e., bulge + outer disk) interpretation.

NGC 4648: Source: Rest et al. (2001). A very clear, strong bar dominates the inner isophotes of the PC image (“misaligned inner structure” in Rest et al.).

NGC 5812: Source: Rest et al. (2001). The light profile is somewhat better fit with a disk + bulge model than by a pure Sérsic model; there is also weak evidence for a possible bar or ring in the $r \approx 2\text{--}5''$ isophotes. This is probably the most uncertain “S0” classification in our rejected set.

NGC 5813: Source: Rest et al. (2001). The ellipticity steadily increases outwards in this galaxy, from ~ 0.1 near the center to ~ 0.3 at large radii, which is possible evidence for an outer disk. Analysis of the light profile indicates a disk + bulge structure as well.

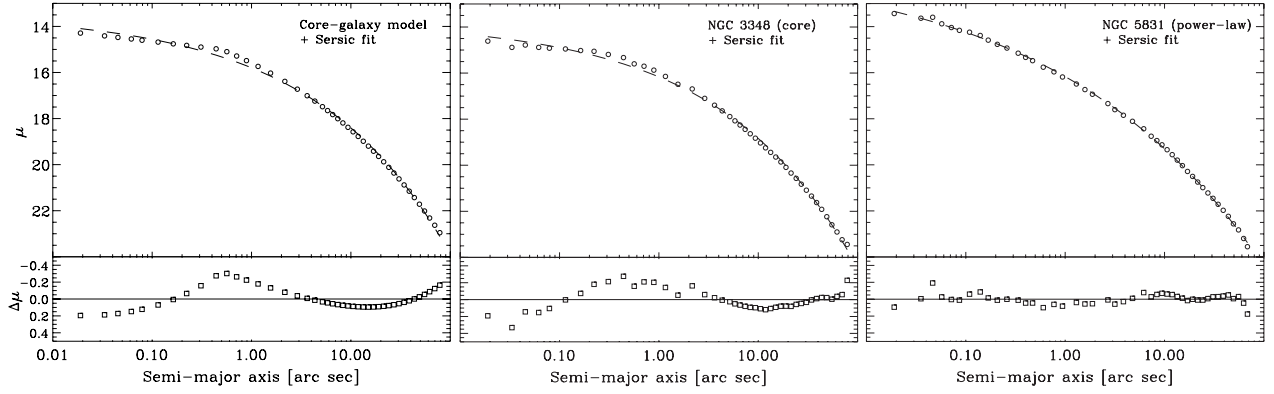


Fig. 3.— How to identify core galaxies using the residuals of a Sérsic fit to the surface-brightness profile. *Left*: a model profile for a core galaxy: a de Vaucouleurs profile ($r_e = 25''$) with a sharp break at $r_b = 0''.5$ to a power-law core with $\gamma = 0.2$. *Middle*: profile of the core galaxy NGC 3348. *Right*: profile of the power-law galaxy NGC 5831. For all three, we also show the best-fitting Sérsic profile (dashed line) and the residuals of the fit (boxes). The characteristic pattern of the residuals (compare model and NGC 3348 versus NGC 5831) indicates a qualitative way of distinguishing core-galaxy profiles.

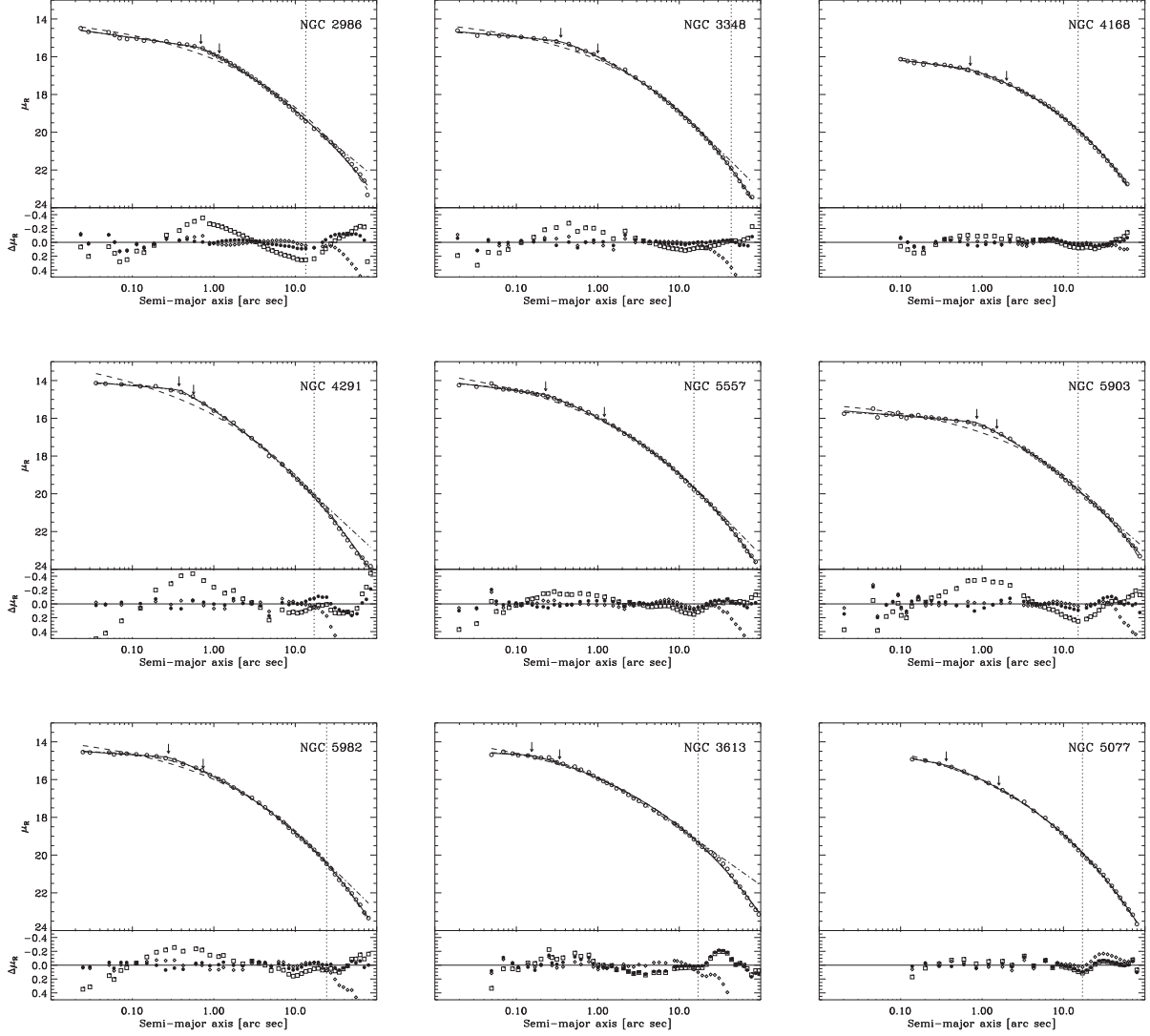


Fig. 4.— Fits to the surface-brightness profiles (open circles) of core galaxies. For each galaxy, we show the best-fitting Sérsic (dashed line) and core-Sérsic (solid line; $\alpha = \infty$ version) models. We also show the best-fitting Nuker-law profiles (dot-dashed line), *fit to the PC part of the profile only*; the outer radius of the Nuker-law fits is marked by the vertical dotted line. Also shown are the residuals for each fit: Sérsic (open squares), core-Sérsic (filled circles), and Nuker (small diamonds). Finally, the break radii of the core-Sérsic (heavy arrow) and Nuker-law (light arrow) fits are indicated. In cases where the break radii of our Nuker-law fits differ significantly from the published fits of Rest et al. (2001), we indicate the *published* value.

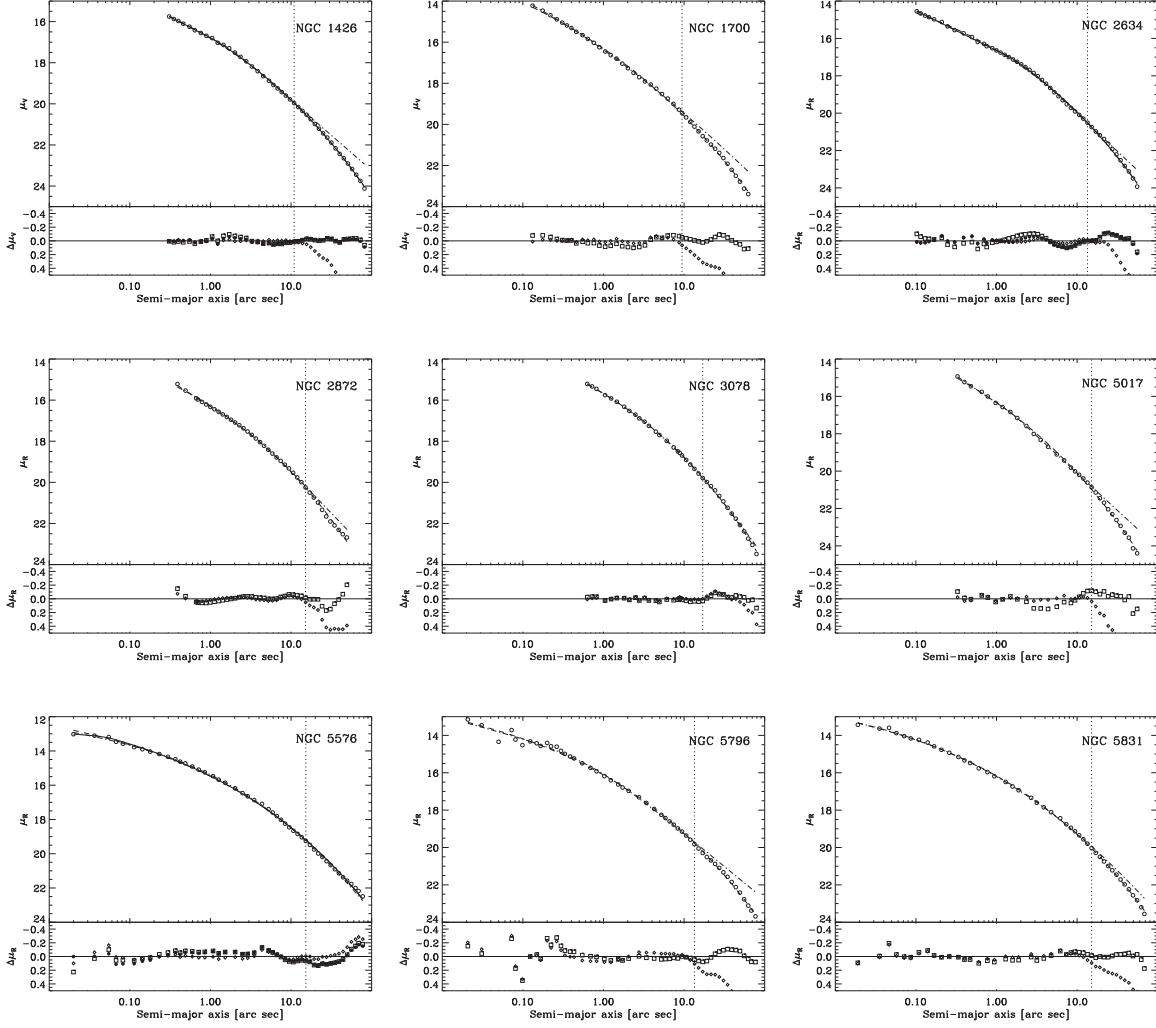


Fig. 5.— As for Figure 4, but showing fits to the surface-brightness profiles of Sérsic (i.e., non-core) galaxies. In several cases, the best core-Sérsic fit is *identical* to the best Sérsic fit, so just the Sérsic and Nuker-law fits are show.

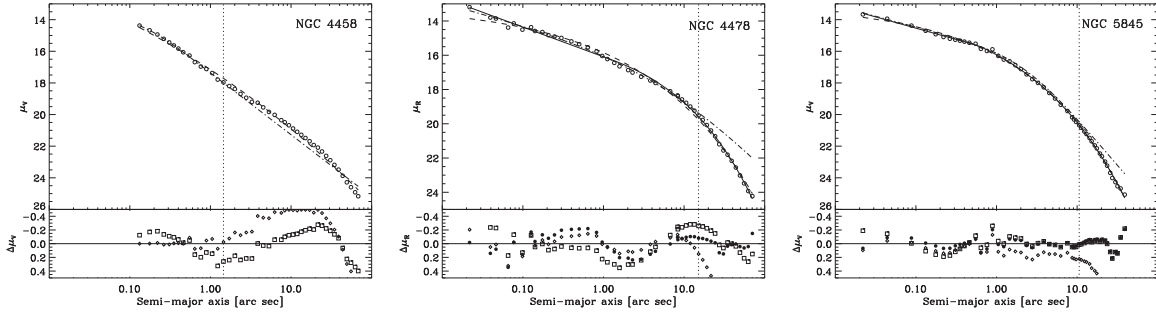


Fig. 6.— As for Figure 5, but showing fits for galaxies with prominent nuclear disks.

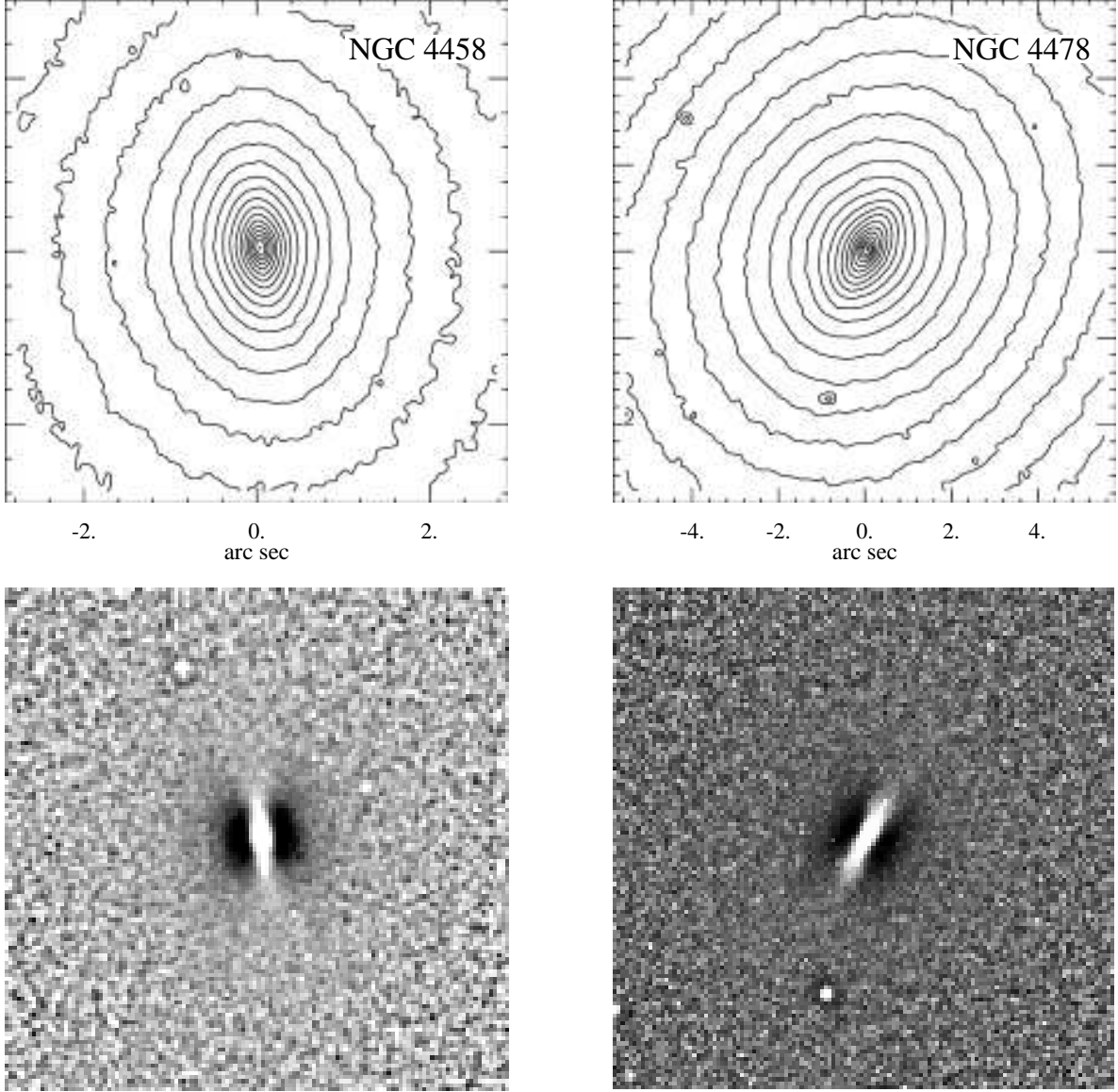


Fig. 7.— Isophote contours (top) and unsharp masks (bottom) of PC images of NGC 4458 and NGC 4478, showing the prominent nuclear disks in each (see also the ellipse fits in Figure 10). These nuclear disks introduce strong deviations from a pure Sérsic models in the surface brightness profiles. (Similar effects are produced by the nuclear disk in NGC 5845; see Quillen, Bowen, & Stritzinger 2000).

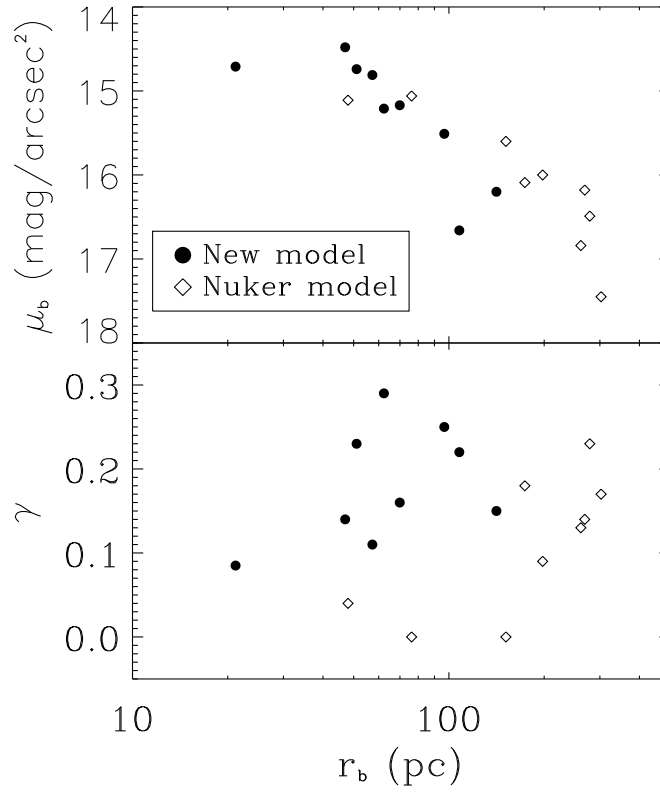


Fig. 8.— Core properties (break radius r_b , inner logarithmic slope γ , and surface brightness at the break radius μ_b) for the core galaxies in our sample. Filled circles are our measurements, using the core-Sérsic fits; open circles are published values from Nuker-law fits Rest et al. (2001).

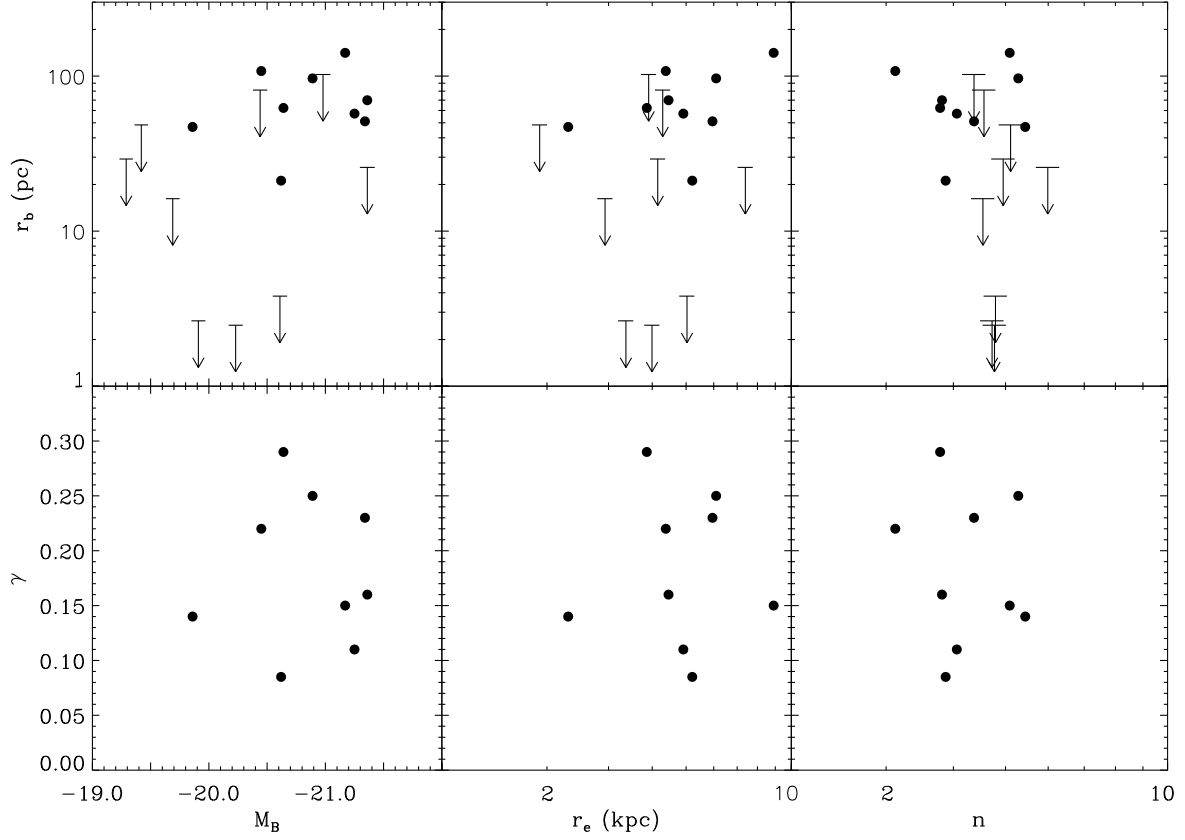


Fig. 9.— Comparison of core properties (break radius r_b and inner logarithmic slope γ) and global properties for the core galaxies in our sample. The upper limits on possible break radii for the Sérsic galaxies (based on the innermost fitted data point; see Column 8 of Table 1) are indicated by the arrows. Three of the latter (NGC 4458, 4478, and 5845) have Sérsic fits that are distorted by bright nuclear disks — see Figures 6 and 7 — so we do not plot their r_e and n values.

Figures for the individual galaxies are available
in the full-resolution version of this paper at:

<http://www.iac.es/galeria/erwin/research/>

Fig. 10.— Isophotes and ellipse fits for WFPC2 mosaic images of the 21 elliptical galaxies in our sample. Contour plots of the isophotes show the entire WFPC2 array; the coordinate axes are centered on the galaxy nucleus. Isophotes are logarithmically scaled and have been smoothed with a 5-pixel-wide median filter prior to contouring. (Due to size constraints, these figures are only available in the full-resolution version of this paper, at: <http://www.iac.es/galeria/erwin/research/>).